

Molecular Gas in the Outskirts

Linda C. Watson and Jin Koda

Abstract The outskirts of galaxies offer extreme environments where we can test our understanding of the formation, evolution, and destruction of molecules and their relationship with star formation and galaxy evolution. We review the basic equations that are used in normal environments to estimate physical parameters like the molecular gas mass from CO line emission and dust continuum emission. Then we discuss how those estimates may be affected when applied to the outskirts, where the average gas density, metallicity, stellar radiation field, and temperature may be lower. We focus on observations of molecular gas in the outskirts of the Milky Way, extragalactic disk galaxies, early-type galaxies, groups, and clusters. The scientific results show the versatility of molecular gas, as it has been used to trace Milky Way spiral arms out to a galactocentric radius of 15 kpc, to study star formation in extended ultraviolet disk galaxies, to probe galaxy interactions in polar ring S0 galaxies, and to investigate ram pressure stripping in clusters. Throughout the Chapter, we highlight the physical stimuli that accelerate the formation of molecular gas, including internal processes such as spiral arm compression and external processes such as interactions.

Linda C. Watson
European Southern Observatory, Alonso de Córdova 3107, Vitacura, Casilla 19001, Santiago, Chile;
e-mail: lwatson@eso.org

Jin Koda
NAOJ Chile Observatory, Joaquín Montero 3000 Oficina 702, Vitacura, Santiago, Chile;
Joint ALMA Office, Alonso de Córdova 3107, Vitacura, Casilla 19001, Santiago, Chile;
Department of Physics and Astronomy, Stony Brook University, Stony Brook, NY 11794, USA;
e-mail: jin.koda@stonybrook.edu

1 Introduction

Despite early discoveries of OB stars and molecular gas in the outer Milky Way (MW; e.g., Fich and Blitz 1984; Brand and Wouterloot 1988), not much attention had been paid to molecular gas in galaxy outskirts primarily because there was a notion that virtually no star formation occurs there. This notion was altered entirely by the *Galaxy Evolution Explorer (GALEX)*, which revealed that ultraviolet emission often extends far beyond the edges of optical disks (namely, extended ultraviolet disks, or XUV disks; Thilker et al 2005; Gil de Paz et al 2007b). The UV emission suggests the presence of massive stars, at least B stars, and hence that there was recent star formation within the lifetime of B stars (~ 100 Myr). These young stars must have been born nearby, perhaps requiring unnoticed molecular gas and clouds somewhere in the extended galaxy outskirts. Average gas densities there are extremely low compared to typical star-forming regions within the MW. Understanding the conditions of parental molecular gas in such an extreme condition is vital to expand our knowledge of the physics of star formation. We need to understand the internal properties of molecular clouds, including the atomic-to-molecular gas phase transition, the distribution of molecular clouds, and the external environment in galaxy outskirts.

A blind search for molecular gas has been difficult for the large outskirts of nearby galaxies due to the limited capability of existing facilities. The Atacama Large Millimeter/submillimeter Array (ALMA) improved the sensitivity remarkably, but even ALMA would need to invest hours to days to carry out a large areal search for molecular gas over extended disks. This review summarizes the current knowledge on molecular gas and star formation in the outskirts, but this research field is still in a phase of discovery. The space to explore is large, and more systematic understanding will become possible with future observations.

Studies of molecular gas in the outskirts will also reveal the yet unknown physical properties of the interstellar medium (ISM) in the outskirts. Most observational tools were developed and calibrated in the inner parts of galactic disks and may not be applicable as they are to the outskirts. Many studies are subject to *systematic biases*, especially when molecular gas in the outskirts is compared with inner disks. For example, the rotational transition of carbon monoxide (CO) is often used to measure the mass of molecular gas in normal galaxies; however, its presence and excitation conditions depend on the metal abundance, stellar radiation field, internal volume and column densities, and kinetic temperature, all of which may change in the outskirts.

In this review, we start from a summary of how the ISM evolves in the inner parts of the MW and nearby galaxies with an emphasis on molecular gas (Sect. 2). We then discuss the observational methods, including the equations needed to plan for a future observational search of molecular gas with a radio telescope (Sect. 3). We explain the potential effects of applying these equations under the extreme conditions in galaxy outskirts, which may cause systematic biases when the ISM is compared between galaxies' inner parts and outskirts (Sect. 3.4). Although not many observations have been carried out in galaxy outskirts, we summarize the current state of

molecular gas observations in spiral (Sect. 4) and elliptical galaxies (Sect. 5) and in galaxy groups and clusters (Sect. 6). We finish the review with possible future directions (Sect. 7). The term “outskirts” is abstract and has been used differently in different contexts. In this review we use this term for the area beyond the optical radius of galaxy, e.g., beyond r_{25} , which is the radius where the B -band surface brightness of a galaxy falls to $25 \text{ mag arcsec}^{-2}$. We should, however, note that in some circumstances r_{25} is not defined well, and we have to rely on a loose definition of “outskirts”.

The measurements of gas properties, such as molecular mass, often depend on some assumptions of the gas properties themselves. However, galaxy outskirts are an extreme environment, and the assumptions based on previous measurements in inner disks may not be appropriate. This problem needs to be resolved iteratively by adjusting the assumptions to match future observations. We therefore spend a number of pages on the methods of basic measurements (Sect. 3), so that the equations and assumptions can be revisited easily in future studies. Readers who already understand the basic methods and assumptions may skip Sect. 3 entirely and move from Sect. 2 to Sect. 4.

2 Molecular Gas from the Inner to the Outer Regions of Galaxies

The most abundant molecule H_2 does not have significant emission at the cold temperatures that are typical in molecular clouds ($< 30 \text{ K}$). Hence, the emission from CO, the second-most abundant molecule, is commonly used to trace molecular gas. Molecular gas is typically concentrated toward the centres of galaxies and its surface density decreases with galactic radius (Young and Scoville 1991; Wong and Blitz 2002). The gas phase changes from mostly molecular in the central regions to more atomic in the outer regions (Sofue et al 1995; Koda et al 2016; Sofue and Nakanishi 2016). These trends apparently continue into the outskirts, as HI disks often extend beyond the edges of optical disks (Bosma 1981).

We may infer the properties of gas in the outskirts by extending our knowledge from the inner disks. Recently, Koda et al (2016) concluded that the HI- H_2 gas phase transition between spiral arm and interarm regions changes as a function of radius in the MW and other nearby galaxies. In the molecule-dominant inner parts, the gas remains highly molecular as it moves from an interarm region into a spiral arm and back into the next interarm region. Stellar feedback does not dissociate molecules much, and perhaps the coagulation and fragmentation of molecular clouds dominate the evolution of the ISM at these radii. The trend differs in the outer regions where the gas phase is atomic on average. The HI gas is converted to H_2 in spiral arm compression and goes back into the HI phase after passing spiral arms. These different regimes of ISM evolution are also seen in the LMC, M33, and M51, depending on the dominant gas phase there (Heyer and Terebey 1998; Engargiola et al 2003; Koda et al 2009; Fukui et al 2009; Tosaki et al 2011; Colombo et al 2014).

Even in regions of relatively low gas densities, a natural fluctuation may occasionally lead to gravitational collapse into molecular gas and clouds. For example, many low-density dwarf galaxies show some molecular gas and star formation. However, some stimulus, such as spiral arm compression, seems necessary to accelerate the HI to H₂ phase transition. In addition to such internal stimuli, there are external stimuli, such as interactions with satellite galaxies, which may also trigger the phase transition into molecular gas in the outskirts.

3 Molecular ISM Masses: Basic Equations

The molecular ISM is typically cold and is observed at radio wavelengths. To search for the molecular ISM in galaxy outskirts one needs to be familiar with conventional notations in radio astronomy. Here we summarize the basic equations and assumptions that have been used in studies of the molecular ISM in traditional environments, such as in the MW's inner disk. In particular, we focus on the $J = 1 - 0, 2 - 1$ rotational transitions of CO molecules and dust continuum emission at millimetre/sub-millimetre wavelengths. The molecular ISM in galaxy outskirts may have different properties from those in the inner disks. We discuss how expected differences could affect the measurements with CO $J = 1 - 0, 2 - 1$, and dust continuum emission.

3.1 Brightness Temperature, Flux Density and Luminosity

The definitions of brightness temperature T_v , brightness I_v , flux density S_v , and luminosity L_v are often confusing. It is useful to go back to the amount of energy (dE) that passes through an aperture (e.g., detector, or sometimes the 4π sky area),

$$dE = I_v d\Omega_B dA dt dv = \{I_v d\Omega_B\} dA dt dv = \{S_v dA\} dt dv = L_v dt dv, \quad (1)$$

where $S_v = \int I_v d\Omega_B$ and $L_v = \int \int I_v d\Omega_B dA$ (see Fig. 1). The dt and dv denote unit time and frequency, respectively. The $d\Omega_B$ is the solid angle of the source and has the relation with the physical area $dB = D^2 d\Omega_B$ with the distance D . Similarly, $dA = D^2 d\Omega_A$ using the solid angle of the aperture area seen from the source $d\Omega_A$. The aperture dA can be a portion of the 4π sky sphere as it is seen from the source and is $4\pi D^2$ when integrated over the entire sphere to calculate luminosity. The dA could also represent an area of a detector (or a pixel of a detector).

The flux density S_v is often expressed in the unit of ‘‘Jansky (Jy)’’, which is equivalent to ‘‘ $10^{-23} \text{ erg s}^{-1} \text{ cm}^{-2} \text{ Hz}^{-1}$ ’’. An integration of I_v over a solid angle $d\Omega_B$ (e.g., telescope beam area or synthesized beam area) provides S_v . In reverse, I_v is S_v divided by the solid angle Ω_B [$= \int d\Omega_B$]. Therefore, the brightness I_v [$= S_v/\Omega_B$] is expressed in the unit of ‘‘Jy/beam’’.

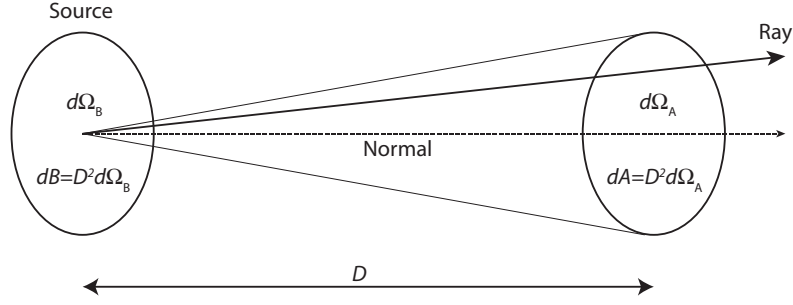


Fig. 1 Definitions of parameters. The rays emitted from the source with the area $dB = D^2 d\Omega_B$ pass through the solid angle $d\Omega_A$ (or the area $D^2 d\Omega_A$) at the distance of D

The brightness temperature T_V is the temperature that makes the black body function $B_\nu(T_V)$ have the same brightness as the observed I_ν at a frequency ν (i.e., $I_\nu = B_\nu(T_V)$), even when I_ν does not follow the black body law! In the Rayleigh-Jeans regime ($h\nu \ll kT$),

$$T_V = \frac{c^2}{2\nu^2 k} I_\nu = \frac{c^2}{2\nu^2 k} \left(\frac{S_\nu}{\Omega_B} \right). \quad (2)$$

The T_V characterizes radiation and is *not necessarily* a physical temperature of an emitting body. However, if the emitting body is an optically thick black body and is filling the beam Ω_B , T_V is equivalent to the physical temperature of the emitting body when the Rayleigh-Jeans criterion is satisfied.

The T_V is measured in ‘‘Kelvin’’. This unit is convenient in radio astronomy since radio single-dish observations calibrate a flux scale in the Kelvin unit using hot and cold loads of known temperatures. Giant molecular clouds (GMCs) in the MW have a typical temperature of ~ 10 K (Scoville and Sanders 1987), and the black body radiation $B_\nu(T)$ at this temperature peaks at $\nu \sim 588$ GHz ($\sim 510 \mu\text{m}$). Therefore, most radio observations of molecular gas are in the Rayleigh-Jeans range.

A numerical expression of Eq. (2) is useful in practice,

$$\left(\frac{T_V}{\text{K}} \right) = 13.6 \left(\frac{\lambda}{\text{mm}} \right)^2 \left(\frac{S_\nu}{\text{Jy}} \right) \left(\frac{b_{\text{maj}} \times b_{\text{min}}}{1'' \times 1''} \right)^{-1}. \quad (3)$$

The last term corresponds to Ω_B in Eq. (2) and is calculated as

$$\Omega_B = \frac{\pi b_{\text{maj}} b_{\text{min}}}{4 \ln 2} \sim 1.133 b_{\text{maj}} b_{\text{min}}, \quad (4)$$

which represents the area of interest (e.g., source size, telescope beam) as a 2-d Gaussian with the major and minor axis FWHM diameters of b_{maj} and b_{min} , respectively. Equation (3) is sometimes written with brightness as

$$\left(\frac{T_v}{\text{K}}\right) = 13.6 \left(\frac{\lambda}{\text{mm}}\right)^2 \left(\frac{I_v}{\text{Jy/beam}}\right) \left(\frac{b_{\text{maj}} \times b_{\text{min}}}{1'' \times 1''}\right)^{-1}, \quad (5)$$

where in this case the last term is for the unit conversion from “beam” into arcsec², and b_{maj} and b_{min} must refer to the telescope beam or synthesized beam.

3.2 Observations of the Molecular ISM using CO Line Emission

Molecular hydrogen (H₂) is the principal component of the ISM at a high density, > 100 cm⁻³. This molecule has virtually no emission at cold temperatures. Hence, CO emission is typically used to trace the molecular ISM. Conventionally, the molecular ISM mass M_{mol} includes the masses of helium and other elements. $M_{\text{mol}} = 1.36 M_{\text{H}_2}$ is used to convert the H₂ mass into M_{mol} .

3.2.1 CO($J = 1 - 0$) Line Emission

The fundamental CO rotational transition $J = 1 - 0$ at $\nu_{\text{CO}}(1-0) = 115.271208 \text{ GHz}$ has been used to measure the molecular ISM mass since the 1980s. For simplicity we omit “CO(1-0)” in subscript and instead write “10”. Hence, $\nu_{\text{CO}}(1-0) = \nu_{10}$.

The dynamical masses of GMCs and their CO(1-0) luminosities are linearly correlated in the MW’s inner disk (Scoville et al 1987; Solomon et al 1987). If a great majority of molecules reside in GMCs, the CO(1-0) luminosity L'_{10} integrated over an area (i.e., an ensemble of GMCs in the area) can be linearly translated to the molecular mass M_{mol} ,

$$M_{\text{mol}} = \alpha_{10} L'_{10}, \quad (6)$$

where α_{10} (or X_{CO} ; see below) is a mass-to-light ratio and is called the CO-to-H₂ conversion factor (Bolatto et al 2013).

By convention we define L'_{10} , instead of L_{10} (Eq.1). With the CO(1-0) brightness temperature T_{10} (instead of I_v or I_{10}), velocity width dv (instead of frequency width $d\nu$), and beam area in physical scale $dB = D^2 d\Omega_B$, it is defined as

$$L'_{10} \equiv \int \int T_{10} dv dB = \frac{c^2}{2\nu_{10}^2 k} \left[\int S_{10} dv \right] D^2, \quad (7)$$

where we used Eq. (2) for T_{10} . The molecular mass is

$$M_{\text{mol}} = \alpha_{10} \frac{c^2}{2\nu_{10}^2 k} \left[\int S_{10} dv \right] D^2. \quad (8)$$

Numerically, this can be expressed as

$$\left(\frac{M_{\text{mol}}}{M_{\odot}}\right) = 1.1 \times 10^4 \left(\frac{\alpha_{10}}{4.3 M_{\odot} \text{pc}^{-2} [\text{K} \cdot \text{km/s}]^{-1}}\right) \left(\frac{\int S_{10} dv}{\text{Jy} \cdot \text{km/s}}\right) \left(\frac{D}{\text{Mpc}}\right)^2. \quad (9)$$

Note that $S_{10} [= \int I_{10} d\Omega_{\text{B}}]$ is an integration over an area of interest (or summation over all pixels within the area). The $\alpha_{10} = 4.3 M_{\odot} \text{pc}^{-2}$ corresponds to the conversion factor of $X_{\text{CO}} = 2.0 \times 10^{20} \text{cm}^{-2} [\text{K} \cdot \text{km/s}]^{-1}$ multiplied by the factor of 1.36 to account for the masses of helium and other elements. α_{10} includes helium, while X_{CO} does not. The calibration of α_{10} (or X_{CO}) is discussed in Bolatto et al (2013).

A typical GMC in the MW has a mass of $4 \times 10^5 M_{\odot}$ and $dv = 8.9 \text{km/s}$ (FWHM) (Scoville and Sanders 1987), which is $\int S_{10} dv \sim 1.5 \text{Jy km/s}$ or $S_{10} \sim 170 \text{mJy}$ at $D = 5 \text{Mpc}$.

3.2.2 CO($J = 2 - 1$) Line Emission

The CO($J = 2 - 1$) emission (230.538 GHz) is also useful for a rough estimation of molecular mass though an excitation condition may play a role (see below). We can redefine Eq. (8) for CO($2 - 1$) by replacing the subscripts from 10 to 21 and using a new CO($2 - 1$)-to- H_2 conversion factor $\alpha_{21} \equiv \alpha_{10}/R_{21/10}$, where $R_{21/10} [\equiv T_{21}/T_{10}]$ is the CO $J = 2 - 1/1 - 0$ line ratio in brightness temperature.

In practice, α_{10} and $R_{21/10}$ are carried over in use of CO($J = 2 - 1$) as these are the parameters that have been measured. Equation (8) is now

$$M_{\text{mol}} = \left(\frac{\alpha_{10}}{R_{21/10}}\right) \frac{c^2}{2v_{21}^2 k} \left[\int S_{21} dv\right] D^2. \quad (10)$$

A numerical evaluation gives

$$\left(\frac{M_{\text{H}_2}}{M_{\odot}}\right) = 3.8 \times 10^3 \left(\frac{\alpha_{10}}{4.3 M_{\odot} \text{pc}^{-2} [\text{K} \cdot \text{km/s}]^{-1}}\right) \left(\frac{R_{21/10}}{0.7}\right)^{-1} \left(\frac{\int S_{21} dv}{\text{Jy} \cdot \text{km/s}}\right) \left(\frac{D}{\text{Mpc}}\right)^2. \quad (11)$$

The typical GMC with $4 \times 10^5 M_{\odot}$ and $dv = 8.9 \text{km/s}$ has $\int S_{21} dv \sim 4.2 \text{Jy km/s}$ or $S_{21} \sim 470 \text{mJy}$ at $D = 5 \text{Mpc}$. Note $S_{21} > S_{10}$ for the same GMC because $S_{21}/S_{10} = (v_{21}/v_{10})^2 T_{21}/T_{10} = (v_{21}/v_{10})^2 R_{21/10} \sim 2.8$ from Eq. (2), where the $(v_{21}/v_{10})^2$ term arises from two facts: (a) each photon carries twice the energy, and (b) there are two times more photons in each frequency interval dv , which is in the denominator of the definition of flux density S . Empirically, $R_{21/10} \sim 0.7$ on average in the MW (Sakamoto et al 1997; Hasegawa 1997), which is consistent with a theoretical explanation under the conditions of the MW disk (Scoville and Solomon 1974; Goldreich and Kwan 1974; see Sect. 3.4).

3.3 Observations of the Molecular ISM using Dust Continuum Emission

Continuum emission from dust provides an alternative means for ISM mass measurement. Dust is mixed in the gas phase ISM, and its emission at millimetre/submillimetre waves correlates well with the fluxes of both atomic gas (HI 21 cm emission) and molecular gas (CO emission). Scoville et al (2016) discussed the usage and calibration of dust emission for ISM mass measurement. We briefly summarize the basic equations, whose normalization will be adjusted with an empirical fitting in the end.

The radiative transfer equation gives the brightness of dust emission

$$I_\nu = (1 - e^{-\tau_\nu})B_\nu(T_d) \quad (12)$$

with the black body radiation $B_\nu(T_d)$ at the dust temperature T_d and the optical depth τ_ν . The flux density of dust is an integration:

$$S_\nu = \int (1 - e^{-\tau_\nu})B_\nu(T_d)d\Omega_B = (1 - e^{-\tau_\nu})B_\nu(T_d)\Omega_B, \quad (13)$$

where B_ν and τ_ν are assumed constant within $\Omega_B [= \int d\Omega_B]$. When the integration is over the beam area, S_ν is the flux density within the beam, and (S_ν/Ω_B) , from Eq. (13), is in Jy/beam.

An integration of S_ν over the entire sky area at the distance of D (i.e., $\int dA = D^2 \int_{4\pi} d\Omega_A = 4\pi D^2$) gives the luminosity

$$L_\nu = \int (1 - e^{-\tau_\nu})B_\nu(T_d)\Omega_B dA = (1 - e^{-\tau_\nu})B_\nu(T_d)\Omega_B 4\pi D^2 \quad (14)$$

$$\approx 4\pi\tau_\nu B_\nu(T_d)D^2\Omega_B = 4\pi\kappa_\nu\Sigma_d B_\nu(T_d)D^2\Omega_B = 4\pi\kappa_\nu M_d B_\nu(T_d). \quad (15)$$

The dust is optically thin at mm/sub-mm wavelengths, and we used $(1 - e^{-\tau_\nu}) \sim \tau_\nu = \kappa_\nu\Sigma_d$, where κ_ν and Σ_d are the absorption coefficient and surface density of dust. The dust mass within the beam is $M_d = \Sigma_d D^2 \Omega_B$. Obviously, the dust continuum luminosity depends on the dust properties (e.g., compositions and size distribution; via κ_ν), amount (M_d), and temperature (T_d).

Equation (15) gives the mass-to-light ratio for dust

$$\frac{M_d}{L_\nu} = \frac{1}{4\pi\kappa_\nu B_\nu(T_d)}. \quad (16)$$

We convert M_d into gas mass, $M_{\text{gas}} = \delta_{\text{GDR}}M_d$, with the gas-to-dust ratio δ_{GDR} . By re-defining the dust absorption coefficient $\kappa'_\nu \equiv \kappa_\nu/\delta_{\text{GDR}}$ (the absorption coefficient per unit total mass of gas), the gas mass-to-dust continuum flux ratio γ_ν at the frequency ν becomes,

$$\gamma_\nu \equiv \frac{M_{\text{gas}}}{L_\nu} = \frac{1}{4\pi\kappa'_\nu B_\nu(T_d)}. \quad (17)$$

Once γ_v is obtained, the gas mass is estimated as $M_{\text{gas}} = \gamma_v L_v$. Here, we use the character γ , instead of α that Scoville et al (2016) used, to avoid a confusion with the CO-to-H₂ conversion factor. Dust continuum emission is associated with HI and H₂, and $M_{\text{gas}} \sim M_{\text{mol}}$ in dense, molecule-dominated regions ($\gtrsim 100 \text{ cm}^{-3}$).

The κ'_v can be approximated as a power-law $\kappa'_v = \kappa'_{850\mu\text{m}} (\lambda/850\mu\text{m})^{-\beta}$ with the spectral index $\beta \sim 1.8$ (Planck Collaboration et al 2011) and coefficient $\kappa'_{850\mu\text{m}}$ at $\lambda = 850\mu\text{m}$ (352 GHz). In order to show the frequency dependence explicitly, we separate $B_v(T_d)$ into the Rayleigh-Jeans term and the correction term $\Gamma_v(T_d)$ as $B_v(T_d) = (2\nu^2 k T_d / c^2) \Gamma_v(T_d)$, where

$$\Gamma_v(T_d) = \frac{x}{e^x - 1} \quad \text{with } x = \frac{h\nu}{kT_d}. \quad (18)$$

Equation (17) has the dependence $\gamma_v \propto \nu^{-(\beta+2)} T_d^{-1} \Gamma_v(T_d)^{-1}$, and the proportionality coefficient, including $\kappa'_{850\mu\text{m}}$ and δ_{GDR} , is evaluated empirically.

Scoville et al (2016) cautioned that T_d should not be derived from a spectral energy distribution fit (which gives a luminosity-weighted average T_d biased toward hot dust with a peak in the infrared). Instead, they suggested to use a mass-weighted T_d for the bulk dust component where the most mass resides. Scoville et al (2016) adopted $T_d = 25 \text{ K}$ and calibrated $\gamma_{v850\mu\text{m}}$ from an empirical comparison of M_{mol} (from CO measurements) and L_v ,

$$\left(\frac{\gamma_v}{M_{\odot} [\text{Jy cm}^2]^{-1}} \right) = 1.5 \pm 0.4 \times 10^3 \left(\frac{\nu}{352 \text{ GHz}} \right)^{-3.8} \left(\frac{T_d}{25 \text{ K}} \right)^{-1} \left(\frac{\Gamma_v(T_d)}{\Gamma_{v850\mu\text{m}}(25 \text{ K})} \right)^{-1}. \quad (19)$$

The luminosity is calculated from the observed S_v in Jy and distance D in centimetre as $L_v = 4\pi D^2 S_v [\text{Jy cm}^2]$. The gas mass is then $M_{\text{mol}} = \gamma_v L_v$.

3.4 The ISM in Extreme Environments Such as the Outskirts

The methods for molecular ISM mass measurement that we discussed above were developed and calibrated mainly for the inner parts of galaxies. However, it is not guaranteed that these calibrations are valid in extreme environments such as galaxy outskirts. In fact, metallicities appear to be lower in the outskirts than in the inner part (see Bresolin, this volume). On a 1 kpc scale average, gas and stellar surface densities, and hence stellar radiation fields, are also lower, although it is not clear if these trends persist at smaller scales, e.g., cloud scales, where the molecular ISM typically exists. Empirically, α_{10} could be larger when metallicities are lower, and $R_{21/10}$ could be smaller when gas density and/or temperature are lower.

In order to search for the molecular ISM and to understand star formation in the outskirts, it is important to take into account the properties and conditions of the ISM there. Here we explain some aspects that may bias measurements if the above equations are applied naively as they are. These potential biases should not

discourage future research, and instead, should be adjusted continuously as we learn more about the ISM in the extreme environment.

3.4.1 Variations of α_{10} (or X_{CO})

The CO-to- H_2 conversion factor α_{10} (or X_{CO}) is a mass-to-light ratio between the CO(1–0) luminosity and the molecular ISM mass (Bolatto et al 2013). Empirically, this factor increases with decreasing metallicity (Arimoto et al 1996; Leroy et al 2011) due to the decreasing abundance of CO over H_2 . At the low metallicity of the small Magellanic cloud ($\sim 1/10Z_{\odot}$), α_{10} appears $\sim 10 - 20$ times larger (Arimoto et al 1996; Leroy et al 2011).

This trend can be understood based on the self-shielding nature of molecular clouds. Molecules on cloud surfaces are constantly photo-dissociated by stellar UV radiation. At high densities within clouds, the formation rate of molecules can be as fast as the dissociation rate, and hence molecules are maintained in molecular clouds. The depth where molecules are maintained depends on the strength of the ambient UV radiation field and its attenuation by line absorptions by the molecules themselves as well as by continuum absorption by dust (van Dishoeck and Black 1988).

H_2 is $\sim 10^4$ times more abundant than CO. It can easily become optically thick on the skin of cloud surfaces and be self-shielded (Fig. 2). On the other hand, UV photons for CO dissociation penetrate deeper into the cloud due to its lower abundance. This process generates the CO-dark H_2 layer around molecular clouds (Fig. 2b; Wolfire et al 2010). Shielding by dust is more important for CO than H_2 . Therefore, if the metallicity or dust abundance is low, the UV photons for CO dissociation reach deeper and deeper, and eventually destroy all CO molecules while H_2 still remains (Fig. 2c). As the CO-dark H_2 layer becomes thicker, L_{10} decreases while M_{H_2} stays high, resulting in a larger α_{10} in a low metallicity environment, such as galaxy outskirts. Since this process depends on the depth that photons can penetrate (through dust attenuation as well as line absorption), the visual extinction A_V is often used as a parameter to characterize α_{10} (or X_{CO}).

3.4.2 Variations of $R_{21/10}$

The CO(2–1) line emission is useful to locate the molecular ISM and to derive a rough estimation of its mass. However, the higher transitions inevitably suffer from excitation conditions. Indeed, $R_{21/10}$ ($\equiv T_{21}/T_{10}$) has been observed to vary by a factor of 2–3 in the MW and in other nearby galaxies, e.g., between star-forming molecular clouds (typically $R_{21/10} \sim 0.7 - 1.0$ and occasionally up to 1.2) and dormant clouds ($\sim 0.4 - 0.7$), and between spiral arms (> 0.7) and inter-arm regions (< 0.7 ; Sakamoto et al 1997; Koda et al 2012). The variation may be negligible for finding molecular gas, but may cause a systematic bias, for example, in comparing galaxy outskirts with inner disks. It is noteworthy that $R_{21/10}$ changes systematically

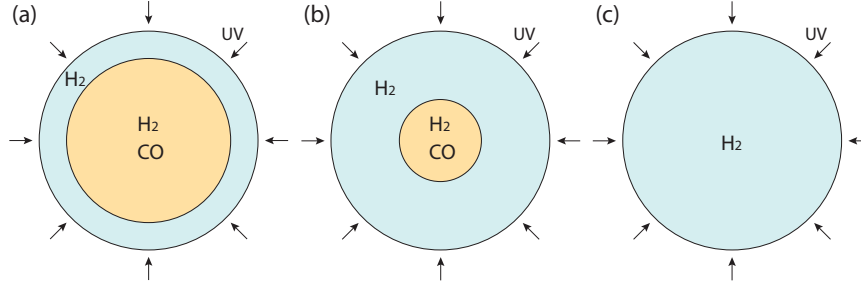


Fig. 2 Self-shielding nature of molecules in molecular clouds. The abundance of molecules is maintained in clouds, since the destruction (photo-dissociation by UV radiation) and formation rates are in balance. The shielding from ambient UV radiation is mainly due to line absorption by molecules themselves. Therefore, the abundant H_2 molecules become optically thick at the absorption line wavelengths on the skin of clouds, while UV photons for CO dissociation can get deeper into clouds. This mechanism generates the CO-dark H_2 layer on the surface of molecular clouds. This layer can become thicker (*panels a, b, c*) under several conditions: e.g., lower metallicity or stronger local radiation field. The CO-to- H_2 conversion factor α_{10} (or X_{CO}) increases with the increasing thickness of the CO-dark H_2 layer, and therefore, with lower metallicity or stronger local radiation field

with star formation activity, and varies along the direction of the Kennicutt-Schmidt relation, which can introduce a bias.

Theoretically, $R_{21/10}$ is controlled by three parameters: the volume density n_{H_2} and kinetic temperature T_{k} – which determine the CO excitation condition due to collisions – and the column density N_{CO} , which controls radiative transfer and photon trapping (Scoville and Solomon 1974; Goldreich and Kwan 1974). Figure 3 shows the variation of $R_{21/10}$ with respect to n_{H_2} and T_{k} under the large velocity gradient (LVG) approximation. In this approximation, the Doppler shift due to a cloud’s internal velocity gradient is assumed to be large enough such that any two parcels along the line of sight do not overlap in velocity space. The front parcel does not block emission from the back parcel, and the optical depth is determined only locally within the parcel (or in small $d\nu$). Therefore, the column density is expressed per velocity $N_{\text{CO}}/d\nu$. A typical velocity range in molecular clouds is adopted for this figure. An average GMC in the MW has $n_{\text{H}_2} \sim 300 \text{ cm}^{-3}$ and $T_{\text{k}} \sim 10 \text{ K}$ (Scoville and Sanders 1987), which results in $R_{21/10}$ of $\sim 0.6 - 0.7$. If the density and/or temperature is a factor of 2 – 3 higher due to a contraction before star formation or feedback from young stars, the ratio increases to $R_{21/10} > 0.7$. On the contrary, if a cloud is dormant compared to the average, the ratio is lower $R_{21/10} < 0.7$.

In the MW, cloud properties appear to change with the galactocentric radius (Heyer and Dame 2015). If their densities or temperatures are lower in the outskirts, it would result in a lower $R_{21/10}$, and hence, a higher H_2 mass at a given CO(2 – 1) luminosity. If the $R_{21/10}$ variation is not accounted for, it could result in a bias when clouds within the inner disk and in the outskirts are compared.

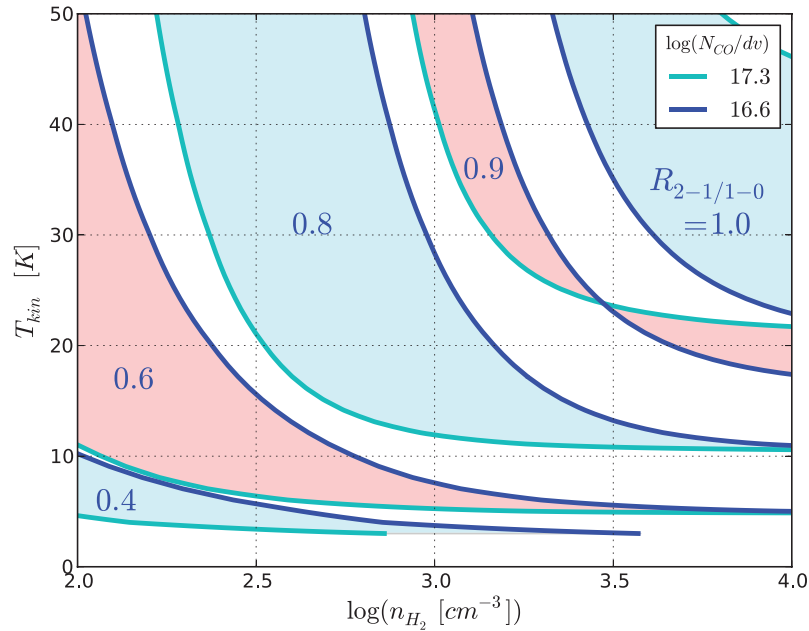


Fig. 3 The CO $J = 2 - 1/1 - 0$ line ratios as function of the gas kinetic temperature T_{kin} and H_2 density n_{H_2} under the LVG approximation (from Koda et al 2012). Most GMCs in the MW have CO column density in the range of $\log(N_{\text{CO}}/dv) \sim 16.6$ to 17.3 , assuming the CO fractional abundance to H_2 of 8×10^{-5} . An average GMC in the MW has $n_{\text{H}_2} \sim 300 \text{ cm}^{-3}$ and $T_{\text{k}} \sim 10 \text{ K}$, and therefore shows $R_{21/10} \sim 0.6-0.7$. $R_{21/10}$ is < 0.7 if the density and/or temperature decrease by a factor of 2–3, and $R_{21/10}$ is > 0.7 if the density and/or temperature increase by a factor of 2–3. Observationally, dormant clouds typically have $R_{21/10} = 0.4 - 0.7$, while actively star forming clouds have $R_{21/10} = 0.7 - 1.0$ (and occasionally up to ~ 1.2 ; Sakamoto et al 1997; Hasegawa 1997). There is also a systematic variation between spiral arms ($R_{21/10} > 0.7$) and interarm regions ($R_{21/10} < 0.7$; Koda et al 2012)

3.4.3 Variations of Dust Properties and Temperature

The gas mass-to-dust luminosity $M_{\text{gas}}/L_{\text{V}}$ depends on the dust properties/emissivity (κ_{V}), dust temperature (T_{d}), and gas-to-dust ratio (δ_{GDR}) – see Eqs. (16) and (17). All of these parameters could change in galaxy outskirts, which have low average metallicity, density, and stellar radiation field. Of course, the assumption of a single T_{d} casts a limitation to the measurement as the ISM is multi-phase in reality, although the key idea of using Eqs. (16) and (17) is to target regions where the cold, molecular ISM is dominant (Scoville et al 2016). The δ_{GDR} may increase with decreasing metallicity by about an order of magnitude ($\delta_{\text{GDR}} \sim 40 \rightarrow 400$) for the change of metallicity $12 + \log(\text{O}/\text{H})$ from $\sim 9.0 \rightarrow 8.0$ (their Fig. 6; Leroy et al

2011). If this trend applies to the outskirts, Eq. (17) would tend to underestimate the gas mass by up to an order of magnitude.

Excess dust emission at millimetre/submillimetre wavelengths has been reported in the small and large Magellanic clouds (SMC and LMC) and other dwarfs (Bot et al 2010; Dale et al 2012; although see also Kirkpatrick et al 2013). This excess emission appears significant when spectral energy distribution fits to infrared data are extrapolated to millimetre/submillimetre wavelengths. Among the possible explanations are the presence of very cold dust, a change of the dust spectral index, and spinning dust emission (e.g., Bot et al 2010). Gordon et al (2014) suggested that variations in the dust emissivity are the most probable cause in the LMC and SMC from their analysis of infrared data from the *Herschel Space Observatory*. The environment of galaxy outskirts may be similar to those of the LMC/SMC. The excess emission (27% and 43% for the LMC and SMC, respectively; Gordon et al 2014) can be ignored if one only needs to locate dust in the vast outskirts, but could cause a systematic bias when the ISM is compared between inner disks and outskirts.

4 Molecular Gas Observations in the Outskirts of Disk Galaxies

A primary motivation for molecular gas observations in the outskirts of disk galaxies has been to study molecular clouds and star formation in an extreme environment with lower average density and metallicity. Many researchers highlight that these studies may teach us about the early Universe, where these conditions were more prevalent.

4.1 The Milky Way

The MW is the disk galaxy with the most molecular gas detections in the outskirts, with pioneering studies of the outer disk molecular gas and star formation properties beginning in the 1980s (e.g., Fich and Blitz 1984; Brand and Wouterloot 1988). The MW can serve as a model for the types of studies that can be done in nearby galaxies with larger and more sensitive facilities. We will use “outer” MW to refer to galactocentric radii between the solar circle ($R_{\text{Gal}} > R_{\odot} = 8.5 \text{ kpc}$) and the edge of the optical disk, which is estimated to be at $R_{\text{Gal}} \sim 13 - 19 \text{ kpc}$ (Ruffle et al 2007; Sale et al 2010 and references therein). We will use “outskirts” to refer to galactocentric radii beyond the edge of the optical disk.

Only about 2% of the molecular mass of the MW is at $R_{\text{Gal}} > 14.5 \text{ kpc}$ (Nakagawa et al 2005 estimated the molecular mass at $R_{\text{Gal}} > 14.5 \text{ kpc}$ to be $2 \times 10^7 M_{\odot}$ while Heyer and Dame 2015 estimated the total molecular mass of the Galaxy to be $(1 \pm 0.3) \times 10^9 M_{\odot}$). N. Izumi (personal communication) collected the known molecular clouds with $R_{\text{Gal}} > 13.5 \text{ kpc}$ in the second and third quadrants (Fig. 4). The molecular cloud with the largest known galactocentric radius is probably Digel

Cloud 1 with a kinematic galactocentric radius of $R_{\text{Gal}} = 22 \text{ kpc}$, dynamical mass of $\sim 6 \times 10^4 M_{\odot}$, and radius of 36 pc (Digel Cloud 2 has a larger kinematic distance of $R_{\text{Gal}} = 24 \text{ kpc}$, but the photometric distance is $R_{\text{Gal}} = 15 - 19 \text{ kpc}$ based on optical spectroscopy of an associated B star; Digel et al 1994; Yasui et al 2006, 2008; Izumi et al 2014). Digel Cloud 1 is beyond the edge of the optical disk but well within the HI disk, which extends to $R_{\text{Gal}} \sim 30 \text{ kpc}$ (Digel et al 1994; Ruffle et al 2007 and references therein).

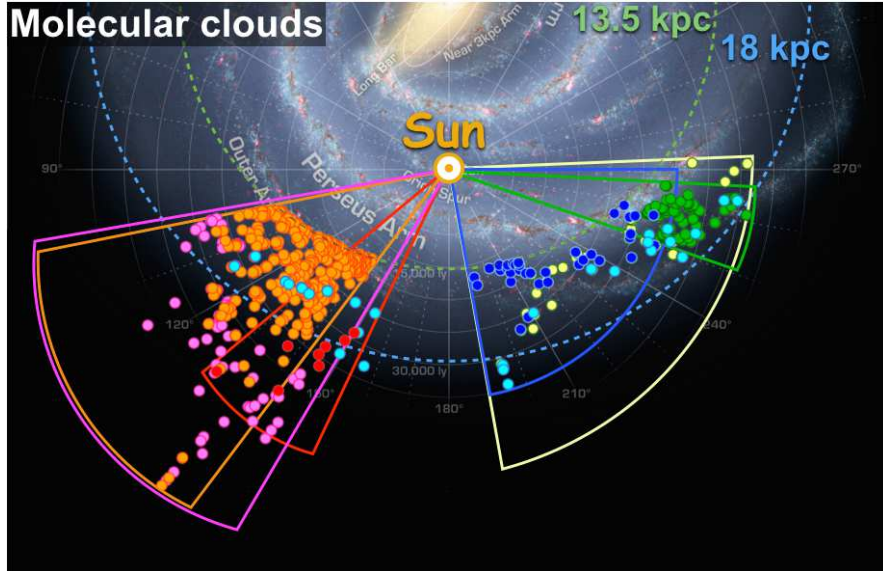


Fig. 4 Figure from N. Izumi (personal communication) showing the known molecular clouds at $R_{\text{Gal}} > 13.5 \text{ kpc}$ in the second and third quadrants overlaid on an artist's conception of the MW (R. Hurt: NASA/JPL-Caltech/SSC). The colours correspond to the following surveys: orange: Brunt et al (2003), magenta: Sun et al (2015), red: Digel et al (1994), cyan: Brand and Wouterloot (1994), blue: May et al (1997), green: Nakagawa et al (2005), yellow: Vázquez et al (2008). The points represent molecular clouds and the fan-shaped regions represent the survey area. The distances were derived assuming $R_{\odot} = 8.5 \text{ kpc}$ and a solar orbital speed of $V_{\odot} = 220 \text{ km s}^{-1}$

Extremely tenuous H_2 gas is mixed with the HI gas in the Galactic halo with a fraction of H_2 over HI of only $10^{-4 \sim -5}$ (Lehner 2002). Such tenuous H_2 is observed via UV absorption, e.g., toward the Magellanic stream (Lehner 2002) and high velocity clouds (HVCs; Bluhm et al 2001). This component is important for understanding the complex physics of the ISM, but is not a major molecular component in galaxy outskirts. We therefore do not discuss this component further in this review.

4.1.1 Properties of Molecular Clouds in the Outer Milky Way

In this Section we highlight studies that have compared the mass, size, and mass surface density of molecular clouds in the outer MW to clouds in the inner MW. Molecular clouds are the site of star formation, and hence, comparisons of their properties between the inner and outer MW is important. In general, molecular clouds in the outer MW have lower mass and mass surface density than clouds in the inner disk. We also describe how molecular clouds have been used to trace spiral arms into the outskirts and to study relatively high-mass star formation.

Heyer and Dame (2015) combined published data on the CO surface brightness out to $R_{\text{Gal}} \sim 20 \text{ kpc}$. The clouds in the outer MW and outskirts are ~ 7 times fainter than clouds in the inner MW (and even fainter relative to the Galactic centre). Assuming a constant X_{CO} , this corresponds to a factor of ~ 7 decrease in the mass surface density of molecular clouds. Heyer and Dame (2015) argued that there is a real decrease in the mass surface density of the molecular clouds, perhaps caused by the lower mid-plane pressure or stronger local FUV radiation field in the outer Galaxy. However, there is also evidence that the outer MW requires a larger X_{CO} to convert the CO surface brightness into the mass surface density (see Sect.3.4). Therefore the mass surface density likely decreases by somewhat less than a factor of ~ 7 .

The mass function of molecular clouds in the outer MW ($9.5 \text{ kpc} \lesssim R_{\text{Gal}} \lesssim 13.5 \text{ kpc}$ in this study) has a steeper power law index than that in the inner MW, such that the outer disk hosts more of its molecular mass in lower-mass clouds (Rosolowsky 2005, based on the 330 deg^2 Heyer et al 1998 catalogue and analysis in Heyer et al 2001 and Brunt et al 2003), although this conclusion may at some level be a result of variable angular resolution (Heyer and Dame 2015). The mass function of the outer MW shows no clear evidence for a truncation at the high-mass end, but under some assumptions Rosolowsky (2005) estimated that the maximum molecular cloud mass is $\sim 2 - 3 \times 10^5 M_{\odot}$. In contrast, Rosolowsky (2005) concluded that the inner MW shows a clear truncation with maximum molecular cloud mass of $\sim 3 \times 10^6 M_{\odot}$. Because of the small number of known clouds, the apparent lack of massive clouds in the outer MW might be due to a sampling effect. This possibility should be addressed in future studies, as a truncation, if it exists, would be an important clue to understanding cloud physics in the outskirts.

Heyer et al (2001) concluded that the size distribution of molecular clouds in the outer MW is similar to the distribution in the inner MW from Solomon et al (1987), but note that surveys with fewer clouds and different galactocentric distance ranges reached different conclusions. May et al (1997) concluded that outer MW clouds have smaller sizes than the inner MW while Brand and Wouterloot (1995) concluded that the outer MW clouds have larger sizes than inner MW clouds at the same mass. While there are conflicting results in the literature, it seems natural to conclude that an outer MW cloud must have a larger radius than an inner MW cloud at the same mass because it appears that the mass surface density of clouds is lower in the outer MW (see above and Heyer and Dame 2015).

Molecular gas observations in the outskirts of the MW have been used to identify spiral arms. Dame and Thaddeus (2011) discovered a spiral arm in the first quadrant at $R_{\text{Gal}} \sim 15$ kpc, based on HI and CO data. Their new arm is consistent with being an extension of the Scutum-Centaurus arm. Sun et al (2015) also used HI and CO data to discover an arm in the second quadrant at $R_{\text{Gal}} = 15 - 19$ kpc. This arm could be a further continuation of the Scutum-Centaurus arm and the Dame and Thaddeus (2011) arm. These kinds of studies are important not only to map the spiral structure of the MW, but also to help understand the observation that star formation in the outskirts of other galaxies often follows spiral arms.

Another important goal of molecular gas studies in the outskirts of the MW has been to understand the connection with star formation under low density and metallicity conditions. For example, Brand and Wouterloot (2007) studied an IRAS-selected molecular cloud with a mass of $4.5 - 6.6 \times 10^3 M_{\odot}$ at $R_{\text{Gal}} \sim 20.2$ kpc. They discovered an embedded cluster of 60 stars and the lack of radio continuum emission limits the most massive star to be later than B0.5. In addition, Kobayashi et al (2008) studied Digel Cloud 2, which is really two clouds each with a mass of $\sim 5 \times 10^3 M_{\odot}$. They discovered embedded clusters in each of the clouds. One cluster likely contains a Herbig Ae/Be star and there are also several Herbig Ae/Be star candidates, a B0-B1 star, and an HII region nearby. Therefore, high-mass star formation has occurred near this low-mass molecular cloud. We encourage more study on the relationship between cloud mass and the most massive star present, as extragalactic studies can trace O and B stars relatively easily, but have difficulty detecting the parent molecular clouds (see Sect. 4.2.1).

In the outskirts of the MW and other galaxies, it is important to ask what triggers molecular cloud and star formation. In Digel Cloud 2, star formation may have been triggered by the expanding HI shell of a nearby supernova remnant (Kobayashi and Tokunaga 2000; Yasui et al 2006; Kobayashi et al 2008) while Izumi et al (2014) hypothesized that the star formation in Digel Cloud 1 may have been triggered by interaction with a nearby HVC.

4.2 Extragalactic Disk Galaxies

We can study molecular gas in more varied environments by moving from the MW to extragalactic disk galaxies. In this Section, we use “outskirts” to refer to galactocentric radii greater than the optical radius ($R_{\text{Gal}} > r_{25}$).

4.2.1 Molecular Gas Detections

Numerous attempts to detect CO beyond the optical radius in the disks of spiral galaxies have failed, although many of the non-detections are unpublished (Watson et al 2016; Morokuma-Matsui et al 2016; J. Braine, F. Combes, J. Donovan Meyer, and A. Gil de Paz, personal communications). To our knowledge, there are

only four isolated spiral galaxies with published CO detections beyond the optical radius (Braine and Herpin 2004; Braine et al 2007, 2010, 2012; Dessauges-Zavadsky et al 2014). Table 1 summarizes the number of detected regions and their range of galactocentric radii and molecular gas masses. Extragalactic studies have not yet reached the molecular gas masses that are typical in the outskirts of the MW ($2 - 20 \times 10^3 M_{\odot}$ for the eleven Digel clouds at $R_{\text{Gal}} = 18 - 22$ kpc; Digel et al 1994; Kobayashi et al 2008; see also Braine et al 2007).

Table 1 Extragalactic disk galaxies in relative isolation with CO detections beyond the optical radius (Braine and Herpin 2004; Braine et al 2007, 2010, 2012; Dessauges-Zavadsky et al 2014). For M33, the molecular gas mass is for one of the detected clouds. For M63, the molecular gas mass is based on a sum of the CO line intensities in twelve pointings, two of which are detections. The NGC 4414, NGC 6946, and M63 masses were computed assuming $X_{\text{CO}} = 2 \times 10^{20} \text{ cm}^{-2} (\text{K km s}^{-1})^{-1}$.

Galaxy	Detected Regions (#)	Galactocentric Radius (r_{25})	Molecular Gas Mass ($10^5 M_{\odot}$)	Method used for Mass
NGC 4414	4	1.1 – 1.5	10 – 20	Within 21" IRAM 30m beam
NGC 6946	4	1.0 – 1.4	1.7 – 3.3	Within 21" IRAM 30m beam
M33	6	1.0 – 1.1	0.43	Virial mass using resolved PdBI data
M63	2	1.36	7.1	Sum of 12 IRAM 30m pointings

It would be useful to be able to predict where CO will be detected in the outskirts of disk galaxies, both as a test of our understanding of the physics of CO formation and destruction in extreme conditions (see Sect. 3.4) and to help us efficiently collect more detections. Most of the published CO studies selected high HI column density regions or regions near young stars traced by $\text{H}\alpha$, FUV, or FIR emission. None of these selection methods is completely reliable. Braine et al (2010) concluded that CO is often associated with large HI and FIR structures, but it is not necessarily located at HI, FIR, or $\text{H}\alpha$ peaks. Many factors might affect the association between HI, CO and star formation tracers. For example, the star forming regions may drift away from their birthplaces over the 10 – 100 Myr timescales traced by $\text{H}\alpha$, FUV, and FIR emission. In addition, feedback from massive stars might destroy molecular clouds more easily in the low-density outskirt environment. Finally, higher-resolution HI maps may show better correlation with CO emission. Sensitive, large-scale ($> \text{kpc}$) maps of the outskirts of disk galaxies may allow for a more impartial study of the conditions that maximize the CO detection rate.

4.2.2 Star Formation in Extragalactic Disk Galaxies

It is generally accepted that stars form from molecular gas (e.g., Fukui and Kawamura 2010) and that an important stage before star formation is the conversion of HI to H_2 (e.g., Leroy et al 2008). A main tool to study the connection between gas and star

formation is the Kennicutt-Schmidt law (Schmidt 1959; Kennicutt 1998), which is an empirical relationship between the star formation rate (SFR) surface density (Σ_{SFR}) and the gas surface density. Within the optical disk of spiral galaxies, there is an approximately linear correlation between Σ_{SFR} and the molecular hydrogen surface density (Σ_{H_2}) but no correlation between Σ_{SFR} and the atomic hydrogen surface density (Σ_{HI} ; e.g., Bigiel et al 2008; Schruba et al 2011).

The majority of the published work connecting the SFR and gas density in the outskirts of disk galaxies has focused on the atomic gas because molecular gas is difficult to detect (Sect. 4.2.1) and because the ISM is dominantly atomic in the outskirts, at least on \gtrsim kpc scales. Bigiel et al (2010) concluded that there is a correlation between the FUV-based Σ_{SFR} and Σ_{HI} in the outskirts of 17 disk galaxies and 5 dwarf galaxies. They measured a longer depletion time in the outskirts, such that it will take on average 10^{11} years to deplete the HI gas reservoir in the outskirts versus 10^9 years to deplete the H_2 gas reservoir within the optical disk. Roychowdhury et al (2015) reached a similar conclusion using HI-dominated regions in disks and dwarfs, including some regions in the outskirts, although they concluded that the depletion time is somewhat shorter than in the outskirts of the Bigiel et al (2010) sample (see also Boissier et al 2007; Dong et al 2008; Barnes et al 2012). The correlation between Σ_{SFR} and Σ_{HI} is surprising because there is no correlation within the optical disk. Bigiel et al (2010) suggested that high HI column density is important for determining where stars will form in the outskirts.

The study of the connection between molecular gas and star formation in the outskirts has been limited by the few molecular gas detections. Figures 5 and 6 show the relationship between Σ_{SFR} and Σ_{H_2} for the molecular gas detections from Table 1 plus a number of deep CO upper limits. In both panels the SFR was computed based on FUV and $24\mu\text{m}$ data to account for the star formation that is unobscured and obscured by dust.

Dessauges-Zavadsky et al (2014) studied a UV-bright region at $r = 1.36 r_{25}$ in the XUV disk of M63 (Fig. 5). They detected CO in two out of twelve pointings and concluded that the molecular gas has a low star formation efficiency (or, equivalently, the molecular gas has a long depletion time) compared to regions within the optical disk. They suggested that the low star formation efficiency may be caused by a warp or by high turbulence. Watson et al (2016) measured a deep CO upper limit in a region at $r = 3.4 r_{25}$ in the XUV disk of NGC 4625 and compiled published CO measurements and upper limits for 15 regions in the XUV disk or outskirts of NGC 4414, NGC 6946, and M33 from Braine and Herpin (2004) and Braine et al (2007, 2010) (see Table 1 and Fig. 6). They concluded that star-forming regions in the outskirts are in general consistent with the same $\Sigma_{\text{SFR}}-\Sigma_{\text{H}_2}$ relationship that exists in the optical disk. However, some points are offset to high star formation efficiency (short depletion time), which may be because the authors selected H α - or FUV-bright regions that could have already exhausted some of the molecular gas supply (as in Schruba et al 2010; Kruijssen and Longmore 2014).

We should ask what stimulates the formation of molecular gas and stars in the outskirts of disk galaxies. Thilker et al (2007) suggested that interactions may trig-

ger the extended star formation in XUV disks while Holwerda et al (2012) suggested that cold accretion may be more important. Bush et al (2008, 2010) carried out hydrodynamic simulations and concluded that spiral density waves can raise the density in an extended gas disk to induce star formation (see also Sect. 4.1.1. of Debattista et al., this volume).

The state-of-the-art data from SINGS (Kennicutt et al 2003), the *GALEX* Nearby Galaxy Survey (Gil de Paz et al 2007a), THINGS (Walter et al 2008), and HERACLES (Leroy et al 2009) brought new insight into the Kennicutt-Schmidt law within the optical disk of spirals. Deeper CO surveys over wider areas in the outskirts could bring a similar increase in our understanding of star formation at the onset of the HI-to-H₂ transition. In such wide-area studies, one should keep in mind that the “standard” physical condition of gas in inner disks could change in the outskirts, which could affect the measurements (Sect. 3.4).

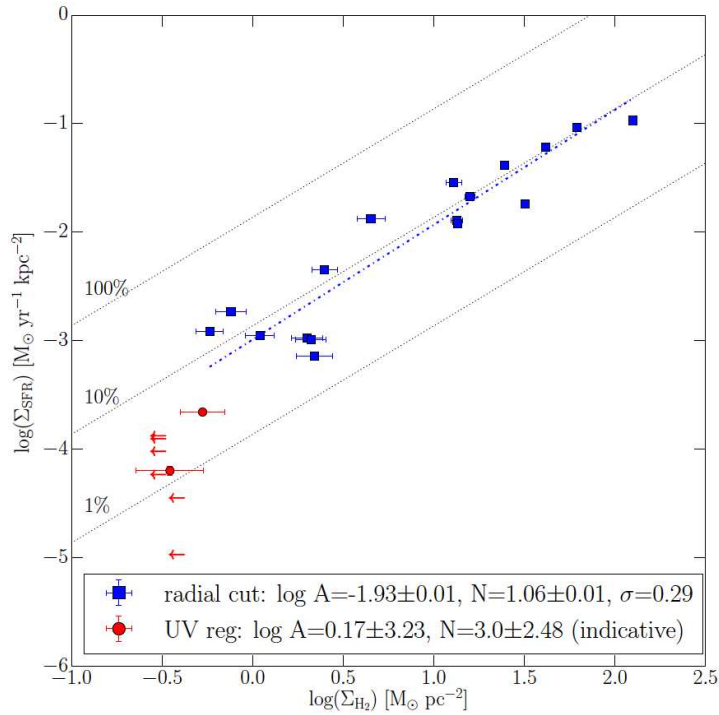


Fig. 5 Figure 7 from Dessauges-Zavadsky et al (2014) showing the molecular-hydrogen Kennicutt-Schmidt relation for the star forming regions in the UV-complex at $r = 1.36 r_{25}$ in M63 (red points) compared to regions within the optical disk (blue points). The blue line shows the fit for the optical disk. The black lines represent constant star formation efficiency, assuming a timescale of 10^8 years. Credit: Dessauges-Zavadsky et al (2014), reproduced with permission © ESO

4.2.3 Theory

This Chapter focuses on observations, but here we briefly highlight theoretical works that are related to molecular gas in the outskirts. The majority of the relevant theoretical studies have concentrated on the origin of gas in the outskirts (e.g., Dekel and Birnboim 2006; Sancisi et al 2008; Sánchez Almeida et al 2014; Mitra et al 2015) and star formation in the outskirts (Bush et al 2008, 2010; Ostriker et al 2010; Krumholz 2013; Sánchez Almeida et al 2014; see also Roškar et al 2010; Khoperskov and Bertin 2015). Krumholz (2013) is particularly relevant because he extended earlier work to develop an analytic model for the atomic and molecular ISM and star formation in outer disks. Krumholz assumed that hydrostatic equilibrium sets the density of cold neutral gas in the outskirts and was able to match the Bigiel et al (2010) observations that show a correlation between Σ_{SFR} and Σ_{HI} (see also Sect. 7 of Elmegreen and Hunter, this volume).

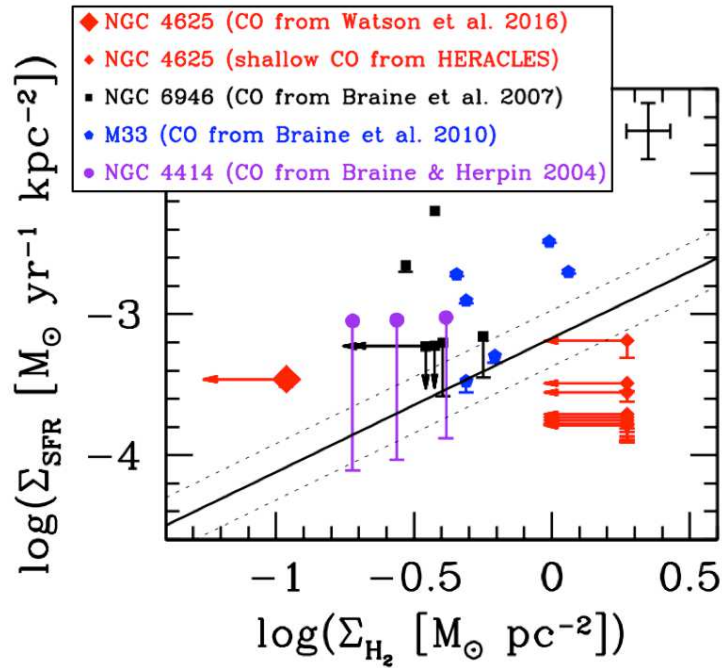


Fig. 6 The molecular hydrogen Kennicutt-Schmidt relation for the remaining star forming regions that are beyond the optical radius in isolated extragalactic disk galaxies and have published CO detections or deep upper limits. The solid line shows the fit for the optical disk of normal spiral galaxies at \sim kpc resolution, with the 1σ scatter shown by the dotted lines (Leroy et al 2013). This figure was originally presented in Fig. 4 in Watson et al (2016)

5 Molecular Gas Observations in the Outskirts of Early-Type Galaxies

Early-type galaxies were historically viewed as “red and dead,” with little gas to form new stars. However, more recent surveys have found reservoirs of cold gas both at galaxy centres and in the outskirts. Molecular gas in the centres of early-type galaxies can have an internal and/or external origin while the molecular gas in the outskirts often originated in a gas-rich companion that has interacted or merged with the early-type. As in all of the environments we have explored, stimuli can also trigger new molecule formation in the outskirts of early-types.

We start with a review of HI in the inner and outer regions of early-type galaxies to put the molecular gas observations in context. The ATLAS^{3D} survey detected HI in 32% of 166 early-type galaxies in a volume-limited sample, down to a 3σ upper limit of $M_{\text{HI}} = 5 \times 10^6 - 5 \times 10^7 M_{\odot}$. Atomic gas in the outskirts of early-type galaxies is even relatively common, as 14% of the ATLAS^{3D} sample have HI that extends out to more than 3.5 times the optical effective radius (Serra et al 2012).

Most surveys of molecular gas in early-type galaxies have focussed on the inner regions. 22% of 260 early-type galaxies in the ATLAS^{3D} sample were detected in CO, down to a 3σ upper limit of $M_{\text{H}_2} \sim 10^7 - 10^8 M_{\odot}$ (Young et al 2011; see also Sage and Wrobel 1989; Knapp and Rupen 1996; Welch and Sage 2003; Combes et al 2007; Welch et al 2010). Within the areas searched, the molecular gas is generally confined to the central few kpc and is distributed in disks, bars plus rings, spiral arms, or with a disrupted morphology (Young 2002; Welch and Sage 2003; Young et al 2008; Davis et al 2013; Alatalo et al 2013).

One important motivation for studies of molecular gas in early-type galaxies has been to determine whether the gas is of internal or external origin. Some of the molecular gas has likely either been present since the galaxies transitioned to being early-type or has accumulated from stellar mass loss (Faber and Gallagher 1976; Young 2002; Young et al 2008; Mathews and Brighenti 2003; Ciotti et al 2010). In contrast, some molecular gas has likely been accreted more recently through minor mergers and/or cold accretion. This external origin is most clearly exhibited by galaxies that display a misalignment between the kinematic axes of the molecular/ionized gas and the stars (Young et al 2008; Crocker et al 2008; Davis et al 2011; Alatalo et al 2013). In particular, Alatalo et al (2013) concluded that 15 galaxies out of a sample of 40 show a kinematic misalignment of at least 30 degrees, which is consistent with gas accretion via minor mergers.

The majority of accreting gas is perhaps in the atomic form, but the outskirts of early-type galaxies also offer the opportunity to study recently accreted molecular gas, which has mainly been detected in polar rings of elliptical and S0 galaxies (see Fig. 7 for an example). These polar rings are present in about 0.5% of nearby S0 galaxies (Whitmore et al 1990). CO has been detected in polar rings at galactocentric radii of 12 kpc in NGC 660 (Combes et al 1992) and 2 kpc in NGC 2685 (Schinnerer and Scoville 2002; see also Watson et al 1994; Galletta et al 1997; Combes et al 2013). Published values for the mass of molecular hydrogen in

the polar rings range from $8 - 11 \times 10^6 M_\odot$ in NGC 2685 (Schinnerer and Scoville 2002) to $10^9 M_\odot$ in NGC 660 (Combes et al 1992), although the handful of polar rings with CO detections are likely biased towards high M_{H_2} .

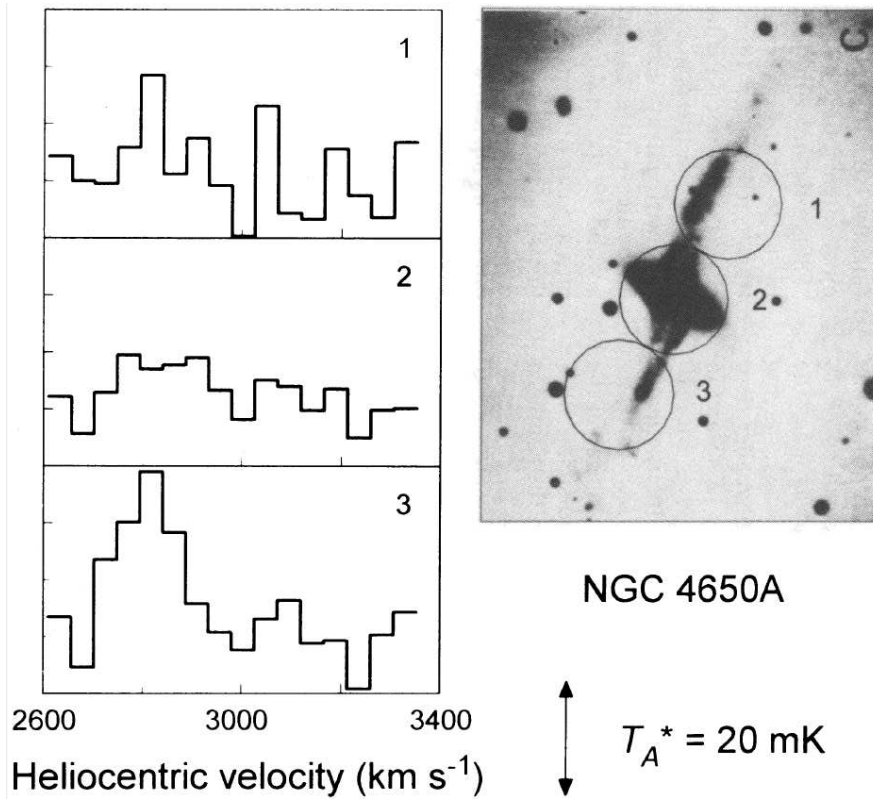


Fig. 7 Figure 2 from Watson et al (1994) showing the Caltech Submillimeter Observatory CO(2 – 1) spectra (*left*) at three pointings, which are indicated by circles in the B-band image of the polar-ring galaxy NGC 4650A (Whitmore et al 1987) on the *right*. Watson et al (1994) estimated the mass of molecular hydrogen in the polar ring of NGC 4650A to be $M_{\text{H}_2} = 8 - 16 \times 10^8 M_\odot$. © AAS. Reproduced with permission

Polar rings are likely caused by tidal accretion from, or a merger with, a gas-rich companion and are stable on timescales of a few Gyr as a result of self gravity (Bournaud and Combes 2003). The molecular gas observations generally support this hypothesis because the molecular gas masses are consistent with those of a dwarf or spiral galaxy (Watson et al 1994; Galletta et al 1997; Schinnerer and Scoville 2002).

Mergers between an early-type galaxy and a gas-rich companion can manifest in non-polar ring systems as well. Buta et al (1995) studied the spheroid-dominated spiral galaxy NGC 7217 and concluded that most of the molecular mass is in an

outer star-forming ring at $R_{\text{Gal}} \sim 0.6 r_{25}$ that could have an H_2 mass that is equal to or greater than the HI mass. More recent work by Sil'chenko et al (2011) indicates that minor mergers may be responsible for the outer ring structures.

Molecular gas has also been detected in shells at a galactocentric radius of 15 kpc ($1.16 r_{25}$) in the elliptical galaxy Centaurus A (Charmandaris et al 2000). Charmandaris et al (2000) calculated the mass of molecular hydrogen in the CenA shells to be $M_{\text{H}_2} = 4.3 \times 10^7 M_{\odot}$. Like polar rings, shells are likely caused by galaxy interactions and Charmandaris et al (2000) concluded that CenA interacted with a massive spiral galaxy rather than a low-mass dwarf galaxy because of the large total gas mass and large ratio of molecular to atomic gas in CenA. Additional molecular cloud formation may have been triggered by the interaction between the shells and the CenA radio jet (see also Salomé et al 2016).

6 Molecular Gas Observations in Galaxy Groups and Clusters

Extended HI gas disks beyond optical edges are common around spiral galaxies, and as already discussed, some stimulus seems necessary to accelerate molecule formation there. In the group/cluster environment, galaxy interactions and interactions with the intergalactic medium (IGM) are triggers for the HI to H_2 phase transition. In the nearby M81 triplet (M82, M81, and NGC 3077), tidal interactions stretch the atomic gas in the outskirts into tidal spiral arms, leading to gravitational collapse to form molecular gas and stars (Brouillet et al 1992; Walter et al 2006). Even an interaction with a minor partner can be a trigger, e.g., in the M51 system, CO emission is detected along the tidal arm/bridge between the main galaxy NGC 5194 and its companion NGC 5195 (Koda et al 2009).

Interaction with the IGM in clusters is also important for the gas phase transition. Most HI gas in galaxy outskirts is stripped away by the ram pressure from the IGM (van Gorkom 2004), while the molecular gas, which resides mostly in inner disks, remains less affected (Kenney and Young 1989; Boselli et al 1997). Some compression acts on the molecular gas near the transition from the molecular-dominant inner disks to the atomic-dominant outer disks, as the extents of molecular disks are smaller when the HI in the outskirts is stripped away (Boselli et al 2014).

The stripped gas in the outskirts is seen as multiphase and has been detected in HI (e.g., Chung et al 2009), $\text{H}\alpha$ (e.g., Yagi et al 2010), and X-rays (e.g., Wang et al 2004; Sun et al 2010). Stripped molecular gas is found in NGC 4438 and NGC 4435, which are interacting galaxies in the Virgo cluster (Vollmer et al 2005). CO emission has also been discovered in the trailing tails of the stripped gas from the disk galaxies ESO137-001 and NGC 4388 in the Norma and Virgo clusters, respectively (Jáchym et al 2014; Verdugo et al 2015).

The ram pressure from the IGM can also heat up and excite H_2 molecules, and H_2 rotational emission lines are detected in the mid-infrared in spiral galaxies in the Virgo cluster (Wong et al 2014). The emission from warm H_2 is also detected over large scales in the intergalactic space of Stephan's Quintet galaxy group with the

Spitzer Space Telescope (Appleton et al 2006). An analysis of the rotational transition ladder of its ground vibrational state suggests the molecular gas has temperatures of 185 ± 30 K and 675 ± 80 K. This H_2 emission coincides with and extends along the X-ray-emitting shock front that is generated by the galaxy NGC 7318b passing through the IGM at a high velocity.

A final example of the cluster environment affecting molecular gas formation is that CO has been detected in cooling flows in the outskirts of galaxies in cluster cores (e.g., Salomé et al 2006). Clearly, the group and cluster environments produce some triggers for the formation of molecular gas in galaxy outskirts and therefore represent another extreme environment where we can test our understanding of the physics of the ISM and star formation.

7 Conclusions and Future Directions

Throughout the Chapter, we have highlighted that some stimuli seem necessary to accelerate the formation of molecular gas in galaxy outskirts. In the outskirts of the MW, stimuli include spiral arm compression, expanding shells from supernova remnants, and interactions with HVCs (Yasui et al 2006; Izumi et al 2014; Koda et al 2016). These same processes are likely at play in the outskirts of extragalactic disk galaxies. In particular, spiral density waves, interactions, and/or cold accretion may stimulate molecule formation and the subsequent star formation activity in XUV disks (Thilker et al 2007; Bush et al 2008; Holwerda et al 2012). Interactions and mergers likely cause the polar rings in the outskirts of S0 galaxies, although it may be more likely that the molecules form in the gas-rich companion before the merger (Bournaud and Combes 2003). Finally, in groups and clusters, interactions and ram pressure stripping may accelerate molecular gas formation in some localized areas of galaxies even as the overall effect is to remove the star-forming fuel from the galaxies (Vollmer et al 2005; Jáchym et al 2014). Galaxy outskirts offer opportunities to study the formation of molecular gas over a variety of conditions and will be the key to understanding if there are different modes of star formation.

Fundamental questions remain about the physical conditions of the ISM in the outskirts. Where is the molecular gas? What are the basic properties of the molecular clouds, e.g., the H_2 volume density, H_2 column density, temperature, mass, and size? How do these properties differ from the properties of molecular clouds in the inner regions of galaxies? Is the transition from HI to H_2 and the transition from H_2 to stars more or less efficient in the outskirts? Are these phase transitions affected by different large-scale processes, stimuli, or environmental conditions compared to inner regions? Measurements of molecular gas properties often depend on assumptions about the gas properties themselves. Right now, those assumptions are based on our knowledge of molecular gas in inner disks. Those assumptions need to be revisited and adjusted continuously as we learn more about molecular gas in the outskirts. This iterative improvement of our knowledge is now starting in the field of galaxy outskirts.

Building on the research that has already been done, we have identified a number of specific studies that would begin to address the fundamental questions above. In the outskirts of the MW, we can study whether the relationship between the mass of the molecular cloud and the most massive associated star is different than in the inner MW. In the outskirts of extragalactic disk galaxies, we need to measure the mass and size functions of molecular clouds and compare to the MW results. In addition, theoretical studies can work towards predicting where and how molecular gas will form in the outskirts. To test these predictions, we encourage sensitive and wide-area mapping of CO and/or dust continuum emission. Higher resolution (cloud-scale) maps of HI may also be required to accurately locate potential sites of molecular gas formation. After each discovery of molecular gas, subsequent multi-wavelength studies including excitation ladders of molecular line emission are necessary to refine our knowledge of the physical conditions of molecular gas there. In early-type galaxies, we should search for molecular gas in XUV disks, as XUV emission could be even more common in early-type galaxies than late-type galaxies (Moffett et al 2012). We hope those researchers will take note and learn from the high failure rate of previous (published and unpublished) searches for molecular gas in the outskirts of disk galaxies.

Acknowledgements We are grateful to Françoise Combes, Jennifer Donovan Meyer, Natsuko Izumi, and Hiroyuki Nakanishi for their advice, reading suggestions, and comments. We also thank Natsuko Izumi for allowing us to use her figure for the distribution of molecular clouds in the outer MW (Fig. 4). JK thanks the NAOJ Chile observatory, a branch of the National Astronomical Observatory of Japan, and the Joint ALMA Observatory for hospitality during his sabbatical visit. JK acknowledges the support from NASA through grant NNX14AF74G.

References

- Alatalo K, Davis TA, Bureau M, Young LM, Blitz L, Crocker AF, Bayet E, Bois M, Bournaud F, Cappellari M, Davies RL, de Zeeuw PT, Duc PA, Emsellem E, Khochfar S, Krajnović D, Kuntschner H, Lablanche PY, Morganti R, McDermid RM, Naab T, Oosterloo T, Sarzi M, Scott N, Serra P, Weijmans AM (2013) The ATLAS^{3D} project - XVIII. CARMA CO imaging survey of early-type galaxies. *MNRAS*432:1796–1844, DOI 10.1093/mnras/sts299, 1210.5524
- Appleton PN, Xu KC, Reach W, Dopita MA, Gao Y, Lu N, Popescu CC, Sulentic JW, Tuffs RJ, Yun MS (2006) Powerful High-Velocity Dispersion Molecular Hydrogen Associated with an Intergalactic Shock Wave in Stephan’s Quintet. *ApJ*639:L51–L54, DOI 10.1086/502646, astro-ph/0602554
- Arimoto N, Sofue Y, Tsujimoto T (1996) CO-to-H₂ Conversion Factor in Galaxies. *PASJ*48:275–284, DOI 10.1093/pasj/48.2.275
- Barnes KL, van Zee L, Côté S, Schade D (2012) Star Formation in the Outer Disk of Spiral Galaxies. *ApJ*757:64, DOI 10.1088/0004-637X/757/1/64
- Bigiel F, Leroy A, Walter F, Brinks E, de Blok WJG, Madore B, Thornley MD (2008) The Star Formation Law in Nearby Galaxies on Sub-Kpc Scales.

- AJ136:2846–2871, DOI 10.1088/0004-6256/136/6/2846, 0810.2541
- Bigiel F, Leroy A, Walter F, Blitz L, Brinks E, de Blok WJG, Madore B (2010) Extremely Inefficient Star Formation in the Outer Disks of Nearby Galaxies. AJ140:1194–1213, DOI 10.1088/0004-6256/140/5/1194, 1007.3498
- Bluhm H, de Boer KS, Marggraf O, Richter P (2001) ORFEUS echelle spectra: Molecular hydrogen in disk, IVC, and HVC gas in front of the LMC. A&A367:299–310, DOI 10.1051/0004-6361:20000346, astro-ph/0012238
- Boissier S, Gil de Paz A, Boselli A, Madore BF, Buat V, Cortese L, Burgarella D, Muñoz-Mateos JC, Barlow TA, Forster K, Friedman PG, Martin DC, Morrissey P, Neff SG, Schiminovich D, Seibert M, Small T, Wyder TK, Bianchi L, Donas J, Heckman TM, Lee YW, Milliard B, Rich RM, Szalay AS, Welsh BY, Yi SK (2007) Radial Variation of Attenuation and Star Formation in the Largest Late-Type Disks Observed with GALEX. ApJS173:524–537, DOI 10.1086/516642, astro-ph/0609071
- Bolatto AD, Wolfire M, Leroy AK (2013) The CO-to-H₂ Conversion Factor. ARA&A51:207–268, DOI 10.1146/annurev-astro-082812-140944, 1301.3498
- Boselli A, Gavazzi G, Lequeux J, Buat V, Casoli F, Dickey J, Donas J (1997) The molecular gas content of spiral galaxies in the Coma/A1367 supercluster. A&A327:522–538
- Boselli A, Cortese L, Boquien M, Boissier S, Catinella B, Gavazzi G, Lagos C, Saintonge A (2014) Cold gas properties of the Herschel Reference Survey. III. Molecular gas stripping in cluster galaxies. A&A564:A67, DOI 10.1051/0004-6361/201322313, 1402.0326
- Bosma A (1981) 21-cm line studies of spiral galaxies. I - Observations of the galaxies NGC 5033, 3198, 5055, 2841, and 7331. II - The distribution and kinematics of neutral hydrogen in spiral galaxies of various morphological types. AJ86:1791–1846, DOI 10.1086/113062
- Bot C, Ysard N, Paradis D, Bernard JP, Lagache G, Israel FP, Wall WF (2010) Submillimeter to centimeter excess emission from the Magellanic Clouds. II. On the nature of the excess. A&A523:A20, DOI 10.1051/0004-6361/201014986, 1008.2875
- Bournaud F, Combes F (2003) Formation of polar ring galaxies. A&A401:817–833, DOI 10.1051/0004-6361:20030150, astro-ph/0301391
- Braine J, Herpin F (2004) Molecular hydrogen beyond the optical edge of an isolated spiral galaxy. Nature432:369–371, DOI 10.1038/nature03054, astro-ph/0412283
- Braine J, Ferguson AMN, Bertoldi F, Wilson CD (2007) The Detection of Molecular Gas in the Outskirts of NGC 6946. ApJ669:L73–L76, DOI 10.1086/524135, 0710.1863
- Braine J, Gratier P, Kramer C, Schuster KF, Tabatabaei F, Gardan E (2010) Molecular cloud formation and the star formation efficiency in M 33. Molecule and star formation in M 33. A&A520:A107, DOI 10.1051/0004-6361/201014166, 1007.0702

- Braine J, Gratier P, Contreras Y, Schuster KF, Brouillet N (2012) A detailed view of a molecular cloud in the far outer disk of M 33. *Molecular cloud formation in M 33*. *A&A*548:A52, DOI 10.1051/0004-6361/201220093, 1210 . 6470
- Brand J, Wouterloot JGA (1988) The velocity field of the outer Galaxy in the southern hemisphere. III - Determination of distances to O, B, and A type stars in the Walraven photometric system. *A&AS*75:117–137
- Brand J, Wouterloot JGA (1994) IRAS sources beyond the solar circle. IV. Maps of far-outer Galaxy molecular clouds. *A&AS*103
- Brand J, Wouterloot JGA (1995) IRAS sources beyond the solar circle. V. Properties of far-outer Galaxy molecular clouds. *A&A*303:851
- Brand J, Wouterloot JGA (2007) A star cluster at the edge of the Galaxy. *A&A*464:909–920, DOI 10.1051/0004-6361:20065437, astro-ph/0702541
- Brouillet N, Henkel C, Baudry A (1992) Detection of an intergalactic molecular complex? *A&A*262:L5–L8
- Brunt CM, Kerton CR, Pomerleau C (2003) An Outer Galaxy Molecular Cloud Catalog. *ApJS*144:47–70, DOI 10.1086/344245
- Bush SJ, Cox TJ, Hernquist L, Thilker D, Younger JD (2008) Simulations of XUV Disks with a Star Formation Density Threshold. *ApJ*683:L13, DOI 10.1086/591523, 0807 . 1116
- Bush SJ, Cox TJ, Hayward CC, Thilker D, Hernquist L, Besla G (2010) Spiral-Induced Star Formation in the Outer Disks of Galaxies. *ApJ*713:780–799, DOI 10.1088/0004-637X/713/2/780, 1003 . 5672
- Buta R, van Driel W, Braine J, Combes F, Wakamatsu K, Sofue Y, Tomita A (1995) NGC 7217: A Spheroid-dominated, Early-Type Resonance Ring Spiral Galaxy. *ApJ*450:593, DOI 10.1086/176169
- Charmandaris V, Combes F, van der Hulst JM (2000) First detection of molecular gas in the shells of CenA. *A&A*356:L1–L4, astro-ph/0003175
- Chung A, van Gorkom JH, Kenney JDP, Crowl H, Vollmer B (2009) VLA Imaging of Virgo Spirals in Atomic Gas (VIVA). I. The Atlas and the H I Properties. *AJ*138:1741–1816, DOI 10.1088/0004-6256/138/6/1741
- Ciotti L, Ostriker JP, Proga D (2010) Feedback from Central Black Holes in Elliptical Galaxies. III. Models with Both Radiative and Mechanical Feedback. *ApJ*717:708–723, DOI 10.1088/0004-637X/717/2/708, 1003 . 0578
- Colombo D, Hughes A, Schinnerer E, Meidt SE, Leroy AK, Pety J, Dobbs CL, García-Burillo S, Dumas G, Thompson TA, Schuster KF, Kramer C (2014) The PdBI Arcsecond Whirlpool Survey (PAWS): Environmental Dependence of Giant Molecular Cloud Properties in M51. *ApJ*784:3, DOI 10.1088/0004-637X/784/1/3, 1401 . 1505
- Combes F, Braine J, Casoli F, Gerin M, van Driel W (1992) Molecular clouds in a polar ring. *A&A*259:L65–L68
- Combes F, Young LM, Bureau M (2007) Molecular gas and star formation in the SAURON early-type galaxies. *MNRAS*377:1795–1807, DOI 10.1111/j.1365-2966.2007.11759.x, astro-ph/0703557
- Combes F, Moiseev A, Reshetnikov V (2013) Molecular content of polar-ring galaxies. *A&A*554:A11, DOI 10.1051/0004-6361/201321385, 1302 . 7273

- Crocker AF, Bureau M, Young LM, Combes F (2008) The molecular polar disc in NGC 2768. *MNRAS*386:1811–1820, DOI 10.1111/j.1365-2966.2008.13177.x, 0803.0426
- Dale DA, Aniano G, Engelbracht CW, Hinz JL, Krause O, Montiel EJ, Roussel H, Appleton PN, Armus L, Beirão P, Bolatto AD, Brandl BR, Calzetti D, Crocker AF, Croxall KV, Draine BT, Galametz M, Gordon KD, Groves BA, Hao CN, Helou G, Hunt LK, Johnson BD, Kennicutt RC, Koda J, Leroy AK, Li Y, Meidt SE, Miller AE, Murphy EJ, Rahman N, Rix HW, Sandstrom KM, Sauvage M, Schinnerer E, Skibba RA, Smith JDT, Tabatabaei FS, Walter F, Wilson CD, Wolfire MG, Zibetti S (2012) Herschel Far-infrared and Submillimeter Photometry for the KINGFISH Sample of nearby Galaxies. *ApJ*745:95, DOI 10.1088/0004-637X/745/1/95, 1112.1093
- Dame TM, Thaddeus P (2011) A Molecular Spiral Arm in the Far Outer Galaxy. *ApJ*734:L24, DOI 10.1088/2041-8205/734/1/L24, 1105.2523
- Davis TA, Alatalo K, Sarzi M, Bureau M, Young LM, Blitz L, Serra P, Crocker AF, Krajnović D, McDermid RM, Bois M, Bournaud F, Cappellari M, Davies RL, Duc PA, de Zeeuw PT, Emsellem E, Khochfar S, Kuntschner H, Lablanche PY, Morganti R, Naab T, Oosterloo T, Scott N, Weijmans AM (2011) The ATLAS^{3D} project - X. On the origin of the molecular and ionized gas in early-type galaxies. *MNRAS*417:882–899, DOI 10.1111/j.1365-2966.2011.19355.x, 1107.0002
- Davis TA, Alatalo K, Bureau M, Cappellari M, Scott N, Young LM, Blitz L, Crocker A, Bayet E, Bois M, Bournaud F, Davies RL, de Zeeuw PT, Duc PA, Emsellem E, Khochfar S, Krajnović D, Kuntschner H, Lablanche PY, McDermid RM, Morganti R, Naab T, Oosterloo T, Sarzi M, Serra P, Weijmans AM (2013) The ATLAS^{3D} Project - XIV. The extent and kinematics of the molecular gas in early-type galaxies. *MNRAS*429:534–555, DOI 10.1093/mnras/sts353, 1211.1011
- Dekel A, Birnboim Y (2006) Galaxy bimodality due to cold flows and shock heating. *MNRAS*368:2–20, DOI 10.1111/j.1365-2966.2006.10145.x, astro-ph/0412300
- Dessauges-Zavadsky M, Verdugo C, Combes F, Pfenniger D (2014) CO map and steep Kennicutt-Schmidt relation in the extended UV disk of M 63. *A&A*566:A147, DOI 10.1051/0004-6361/201323330, 1406.0310
- Digel S, de Geus E, Thaddeus P (1994) Molecular clouds in the extreme outer galaxy. *ApJ*422:92–101, DOI 10.1086/173706
- Dong H, Calzetti D, Regan M, Thilker D, Bianchi L, Meurer GR, Walter F (2008) Spitzer Observations of Star Formation in the Extreme Outer Disk of M83 (NGC5236). *AJ*136:479–497, DOI 10.1088/0004-6256/136/1/479, 0804.3632
- Engargiola G, Plambeck RL, Rosolowsky E, Blitz L (2003) Giant Molecular Clouds in M33. I. BIMA All-Disk Survey. *ApJS*149:343–363, DOI 10.1086/379165, arXiv:astro-ph/0308388
- Faber SM, Gallagher JS (1976) H I in early-type galaxies. II - Mass loss and galactic winds. *ApJ*204:365–375, DOI 10.1086/154180
- Fich M, Blitz L (1984) Optical H II regions in the outer galaxy. *ApJ*279:125–135, DOI 10.1086/161872

- Fukui Y, Kawamura A (2010) Molecular Clouds in Nearby Galaxies. *ARA&A*48:547–580, DOI 10.1146/annurev-astro-081309-130854
- Fukui Y, Kawamura A, Wong T, Murai M, Iritani H, Mizuno N, Mizuno Y, Onishi T, Hughes A, Ott J, Muller E, Staveley-Smith L, Kim S (2009) Molecular and Atomic Gas in the Large Magellanic Cloud. II. Three-dimensional Correlation Between CO and H I. *ApJ*705:144–155, DOI 10.1088/0004-637X/705/1/144, 0909.0382
- Galletta G, Sage LJ, Sparke LS (1997) Molecular gas in polar-ring galaxies. *MNRAS*284:773–784, DOI 10.1093/mnras/284.3.773
- Gil de Paz A, Boissier S, Madore BF, Seibert M, Joe YH, Boselli A, Wyder TK, Thilker D, Bianchi L, Rey SC, Rich RM, Barlow TA, Conrow T, Forster K, Friedman PG, Martin DC, Morrissey P, Neff SG, Schiminovich D, Small T, Donas J, Heckman TM, Lee YW, Milliard B, Szalay AS, Yi S (2007a) The GALEX Ultraviolet Atlas of Nearby Galaxies. *ApJS*173:185–255, DOI 10.1086/516636, astro-ph/0606440
- Gil de Paz A, Madore BF, Boissier S, Thilker D, Bianchi L, Sánchez Contreras C, Barlow TA, Conrow T, Forster K, Friedman PG, Martin DC, Morrissey P, Neff SG, Rich RM, Schiminovich D, Seibert M, Small T, Donas J, Heckman TM, Lee YW, Milliard B, Szalay AS, Wyder TK, Yi S (2007b) Chemical and Photometric Evolution of Extended Ultraviolet Disks: Optical Spectroscopy of M83 (NGC 5236) and NGC 4625. *ApJ*661:115–134, DOI 10.1086/513730, arXiv:astro-ph/0702302
- Goldreich P, Kwan J (1974) Molecular Clouds. *ApJ*189:441–454, DOI 10.1086/152821
- Gordon KD, Roman-Duval J, Bot C, Meixner M, Babler B, Bernard JP, Bolatto A, Boyer ML, Clayton GC, Engelbracht C, Fukui Y, Galametz M, Galliano F, Hony S, Hughes A, Indebetouw R, Israel FP, Jameson K, Kawamura A, Lebouteiller V, Li A, Madden SC, Matsuura M, Misselt K, Montiel E, Okumura K, Onishi T, Panuzzo P, Paradis D, Rubio M, Sandstrom K, Sauvage M, Seale J, Sewiło M, Tchernyshyov K, Skibba R (2014) Dust and Gas in the Magellanic Clouds from the HERITAGE Herschel Key Project. I. Dust Properties and Insights into the Origin of the Submillimeter Excess Emission. *ApJ*797:85, DOI 10.1088/0004-637X/797/2/85, 1406.6066
- Hasegawa T (1997) The CO 2-1/1-0 ratio. In: W B Latter, S J E Radford, P R Jewell, J G Mangum, & J Bally (ed) *IAU Symposium*, IAU Symposium, vol 170, pp 39–46
- Heyer M, Dame TM (2015) Molecular Clouds in the Milky Way. *ARA&A*53:583–629, DOI 10.1146/annurev-astro-082214-122324
- Heyer MH, Terebey S (1998) The Anatomy of the Perseus Spiral Arm: ^{12}CO and IRAS Imaging Observations of the W3-W4-W5 Cloud Complex. *ApJ*502:265–277, DOI 10.1086/305881
- Heyer MH, Brunt C, Snell RL, Howe JE, Schloerb FP, Carpenter JM (1998) The Five College Radio Astronomy Observatory CO Survey of the Outer Galaxy. *ApJS*115:241–258, DOI 10.1086/313086

- Heyer MH, Carpenter JM, Snell RL (2001) The Equilibrium State of Molecular Regions in the Outer Galaxy. *ApJ*551:852–866, DOI 10.1086/320218, astro-ph/0101133
- Holwerda BW, Pirzkal N, Heiner JS (2012) Quantified H I morphology - VI. The morphology of extended discs in UV and H I. *MNRAS*427:3159–3175, DOI 10.1111/j.1365-2966.2012.21975.x, 1207.4916
- Izumi N, Kobayashi N, Yasui C, Tokunaga AT, Saito M, Hamano S (2014) Discovery of Star Formation in the Extreme Outer Galaxy Possibly Induced by a High-velocity Cloud Impact. *ApJ*795:66, DOI 10.1088/0004-637X/795/1/66, 1411.7290
- Jáchym P, Combes F, Cortese L, Sun M, Kenney JDP (2014) Abundant Molecular Gas and Inefficient Star Formation in Intracluster Regions: Ram Pressure Stripped Tail of the Norma Galaxy ESO137-001. *ApJ*792:11, DOI 10.1088/0004-637X/792/1/11, 1403.2328
- Kenney JDP, Young JS (1989) The effects of environment on the molecular and atomic gas properties of large Virgo cluster spirals. *ApJ*344:171–199, DOI 10.1086/167787
- Kennicutt RC Jr (1998) The Global Schmidt Law in Star-forming Galaxies. *ApJ*498:541–552, DOI 10.1086/305588, astro-ph/9712213
- Kennicutt RC Jr, Armus L, Bendo G, Calzetti D, Dale DA, Draine BT, Engelbracht CW, Gordon KD, Grauer AD, Helou G, Hollenbach DJ, Jarrett TH, Kewley LJ, Leitherer C, Li A, Malhotra S, Regan MW, Rieke GH, Rieke MJ, Roussel H, Smith JD, Thornley MD, Walter F (2003) SINGS: The SIRTf Nearby Galaxies Survey. *PASP*115:928–952, DOI 10.1086/376941, astro-ph/0305437
- Khoperskov SA, Bertin G (2015) Spiral density waves in the outer galactic gaseous discs. *MNRAS*451:2889–2899, DOI 10.1093/mnras/stv1145, 1505.04598
- Kirkpatrick A, Calzetti D, Galametz M, Kennicutt R Jr, Dale D, Aniano G, Sandstrom K, Armus L, Crocker A, Hinz J, Hunt L, Koda J, Walter F (2013) Investigating the Presence of 500 μm Submillimeter Excess Emission in Local Star Forming Galaxies. *ApJ*778:51, DOI 10.1088/0004-637X/778/1/51, 1310.0456
- Knapp GR, Rupen MP (1996) Molecular Gas in Elliptical Galaxies: CO Observations of an IRAS Flux-limited Sample. *ApJ*460:271, DOI 10.1086/176967
- Kobayashi N, Tokunaga AT (2000) Discovery of Young Stellar Objects at the Edge of the Optical Disk of Our Galaxy. *ApJ*532:423–429, DOI 10.1086/308564, astro-ph/9909327
- Kobayashi N, Yasui C, Tokunaga AT, Saito M (2008) Star Formation in the Most Distant Molecular Cloud in the Extreme Outer Galaxy: A Laboratory of Star Formation in an Early Epoch of the Galaxy's Formation. *ApJ*683:178–188, DOI 10.1086/588421, 0803.3369
- Koda J, Scoville N, Sawada T, La Vigne MA, Vogel SN, Potts AE, Carpenter JM, Corder SA, Wright MCH, White SM, Zauderer BA, Patience J, Sargent AI, Bock DCJ, Hawkins D, Hodges M, Kembell A, Lamb JW, Plambeck RL, Pound MW, Scott SL, Teuben P, Woody DP (2009) Dynamically Driven Evolution of the Interstellar Medium in M51. *ApJ*700:L132–L136, DOI 10.1088/0004-637X/700/2/L132, 0907.1656

- Koda J, Scoville N, Hasegawa T, Calzetti D, Donovan Meyer J, Egusa F, Kennicutt R, Kuno N, Louie M, Momose R, Sawada T, Sorai K, Umei M (2012) Physical Conditions in Molecular Clouds in the Arm and Interarm Regions of M51. *ApJ*761:41, DOI 10.1088/0004-637X/761/1/41, 1210 . 6349
- Koda J, Scoville N, Heyer M (2016) Evolution of Molecular and Atomic Gas Phases in the Milky Way. *ApJ*823:76, DOI 10.3847/0004-637X/823/2/76, 1604 . 01053
- Kruijssen JMD, Longmore SN (2014) An uncertainty principle for star formation - I. Why galactic star formation relations break down below a certain spatial scale. *MNRAS*439:3239–3252, DOI 10.1093/mnras/stu098, 1401 . 4459
- Krumholz MR (2013) The star formation law in molecule-poor galaxies. *MNRAS*436:2747–2762, DOI 10.1093/mnras/stt1780, 1309 . 5100
- Lehner N (2002) Far-Ultraviolet Spectroscopic Explorer Observations of the Magellanic Bridge Gas toward Two Early-Type Stars: Molecules, Physical Conditions, and Relative Abundances. *ApJ*578:126–143, DOI 10.1086/342349, astro-ph/0206250
- Leroy AK, Walter F, Brinks E, Bigiel F, de Blok WJG, Madore B, Thornley MD (2008) The Star Formation Efficiency in Nearby Galaxies: Measuring Where Gas Forms Stars Effectively. *AJ*136:2782–2845, DOI 10.1088/0004-6256/136/6/2782, 0810 . 2556
- Leroy AK, Walter F, Bigiel F, Usero A, Weiss A, Brinks E, de Blok WJG, Kennicutt RC, Schuster KF, Kramer C, Wiesemeyer HW, Roussel H (2009) Heracles: The HERA CO Line Extragalactic Survey. *AJ*137:4670–4696, DOI 10.1088/0004-6256/137/6/4670, 0905 . 4742
- Leroy AK, Bolatto A, Gordon K, Sandstrom K, Gratier P, Rosolowsky E, Engelbracht CW, Mizuno N, Corbelli E, Fukui Y, Kawamura A (2011) The CO-to-H₂ Conversion Factor from Infrared Dust Emission across the Local Group. *ApJ*737:12, DOI 10.1088/0004-637X/737/1/12, 1102 . 4618
- Leroy AK, Walter F, Sandstrom K, Schrubba A, Munoz-Mateos JC, Bigiel F, Bolatto A, Brinks E, de Blok WJG, Meidt S, Rix HW, Rosolowsky E, Schinnerer E, Schuster KF, Usero A (2013) Molecular Gas and Star Formation in nearby Disk Galaxies. *AJ*146:19, DOI 10.1088/0004-6256/146/2/19, 1301 . 2328
- Mathews WG, Brighenti F (2003) Hot Gas in and around Elliptical Galaxies. *ARA&A*41:191–239, DOI 10.1146/annurev.astro.41.090401.094542, astro-ph/0309553
- May J, Alvarez H, Bronfman L (1997) Physical properties of molecular clouds in the southern outer Galaxy. *A&A*327:325–332
- Mitra S, Davé R, Finlator K (2015) Equilibrium model constraints on baryon cycling across cosmic time. *MNRAS*452:1184–1200, DOI 10.1093/mnras/stv1387, 1411 . 1157
- Moffett AJ, Kannappan SJ, Baker AJ, Laine S (2012) Extended Ultraviolet Disks and Ultraviolet-bright Disks in Low-mass E/S0 Galaxies. *ApJ*745:34, DOI 10.1088/0004-637X/745/1/34, 1111 . 0959
- Morokuma-Matsui K, Koda J, Takekoshi T, Saito M, Nakanishi H, Boissier S, Madore B, Boselli A, Gil de Paz A, Thilker D, Yagi M, Sorai K, Kuno N

- (2016) Search for molecular gas in XUV disk of M83. In: Gil de Paz A, Lee JC, Knapen JH (eds) Proceedings of IAU Symposium 321, "Formation and evolution of galaxy outskirts", Cambridge University Press, Cambridge
- Nakagawa M, Onishi T, Mizuno A, Fukui Y (2005) An Unbiased Search for Molecular Clouds in the Southern Galactic Warp. PASJ57:917–931, DOI 10.1093/pasj/57.6.917, astro-ph/0510473
- Ostriker EC, McKee CF, Leroy AK (2010) Regulation of Star Formation Rates in Multiphase Galactic Disks: A Thermal/Dynamical Equilibrium Model. ApJ721:975–994, DOI 10.1088/0004-637X/721/2/975, 1008.0410
- Planck Collaboration, Ade PAR, Aghanim N, Arnaud M, Ashdown M, Aumont J, Baccigalupi C, Balbi A, Banday AJ, Barreiro RB, et al (2011) Planck early results. XIX. All-sky temperature and dust optical depth from Planck and IRAS. Constraints on the "dark gas" in our Galaxy. A&A536:A19, DOI 10.1051/0004-6361/201116479, 1101.2029
- Rosolowsky E (2005) The Mass Spectra of Giant Molecular Clouds in the Local Group. PASP117:1403–1410, DOI 10.1086/497582, astro-ph/0508679
- Roškar R, Debattista VP, Brooks AM, Quinn TR, Brook CB, Governato F, Dalcanton JJ, Wadsley J (2010) Misaligned angular momentum in hydrodynamic cosmological simulations: warps, outer discs and thick discs. MNRAS408:783–796, DOI 10.1111/j.1365-2966.2010.17178.x, 1006.1659
- Roychowdhury S, Huang ML, Kauffmann G, Wang J, Chengalur JN (2015) The spatially resolved Kennicutt-Schmidt relation in the H I-dominated regions of spiral and dwarf irregular galaxies. MNRAS449:3700–3709, DOI 10.1093/mnras/stv515, 1503.02667
- Ruffle PME, Millar TJ, Roberts H, Lubowich DA, Henkel C, Pasachoff JM, Brammer G (2007) Galactic Edge Clouds. I. Molecular Line Observations and Chemical Modeling of Edge Cloud 2. ApJ671:1766–1783, DOI 10.1086/522775, 0708.2740
- Sage LJ, Wrobel JM (1989) Detection of CO emission from S0 galaxies. ApJ344:204–209, DOI 10.1086/167789
- Sakamoto S, Hasegawa T, Handa T, Hayashi M, Oka T (1997) An Out-of-Plane CO ($J = 2-1$) Survey of the Milky Way. II. Physical Conditions of Molecular Gas. ApJ486:276, DOI 10.1086/304479
- Sale SE, Drew JE, Knigge C, Zijlstra AA, Irwin MJ, Morris RAH, Phillipps S, Drake JJ, Greimel R, Unruh YC, Groot PJ, Mampaso A, Walton NA (2010) The structure of the outer Galactic disc as revealed by IPHAS early A stars. MNRAS402:713–723, DOI 10.1111/j.1365-2966.2009.15746.x, 0909.3857
- Salomé P, Combes F, Edge AC, Crawford C, Erlund M, Fabian AC, Hatch NA, Johnstone RM, Sanders JS, Wilman RJ (2006) Cold molecular gas in the Perseus cluster core. Association with X-ray cavity, H α filaments and cooling flow. A&A454:437–445, DOI 10.1051/0004-6361:20054745, astro-ph/0603350
- Salomé Q, Salomé P, Combes F, Hamer S, Heywood I (2016) Star formation efficiency along the radio jet in Centaurus A. A&A586:A45, DOI 10.1051/0004-6361/201526409, 1511.04310

- Sánchez Almeida J, Elmegreen BG, Muñoz-Tuñón C, Elmegreen DM (2014) Star formation sustained by gas accretion. *A&A Rev.*22:71, DOI 10.1007/s00159-014-0071-1, 1405.3178
- Sancisi R, Fraternali F, Oosterloo T, van der Hulst T (2008) Cold gas accretion in galaxies. *A&A Rev.*15:189–223, DOI 10.1007/s00159-008-0010-0, 0803.0109
- Schinnerer E, Scoville N (2002) First Interferometric Observations of Molecular Gas in a Polar Ring: The Helix Galaxy NGC 2685. *ApJ*577:L103–L106, DOI 10.1086/344242, astro-ph/0209004
- Schmidt M (1959) The Rate of Star Formation. *ApJ*129:243, DOI 10.1086/146614
- Schruba A, Leroy AK, Walter F, Sandstrom K, Rosolowsky E (2010) The Scale Dependence of the Molecular Gas Depletion Time in M33. *ApJ*722:1699–1706, DOI 10.1088/0004-637X/722/2/1699, 1009.1651
- Schruba A, Leroy AK, Walter F, Bigiel F, Brinks E, de Blok WJG, Dumas G, Kramer C, Rosolowsky E, Sandstrom K, Schuster K, Usero A, Weiss A, Wiesemeyer H (2011) A Molecular Star Formation Law in the Atomic-gas-dominated Regime in Nearby Galaxies. *AJ*142:37, DOI 10.1088/0004-6256/142/2/37, 1105.4605
- Scoville N, Sheth K, Aussel H, Vanden Bout P, Capak P, Bongiorno A, Casey CM, Murchikova L, Koda J, Álvarez-Márquez J, Lee N, Laigle C, McCracken HJ, Ilbert O, Pope A, Sanders D, Chu J, Toft S, Ivison RJ, Manohar S (2016) ISM Masses and the Star formation Law at $Z = 1$ to 6: ALMA Observations of Dust Continuum in 145 Galaxies in the COSMOS Survey Field. *ApJ*820:83, DOI 10.3847/0004-637X/820/2/83, 1511.05149
- Scoville NZ, Sanders DB (1987) H₂ in the Galaxy. In: D J Hollenbach & H A Thronson Jr (ed) *Interstellar Processes, Astrophysics and Space Science Library*, vol 134, pp 21–50
- Scoville NZ, Solomon PM (1974) Radiative Transfer, Excitation, and Cooling of Molecular Emission Lines (co and Cs). *ApJ*187:L67, DOI 10.1086/181398
- Scoville NZ, Yun MS, Sanders DB, Clemens DP, Waller WH (1987) Molecular clouds and cloud cores in the inner Galaxy. *ApJS*63:821–915, DOI 10.1086/191185
- Serra P, Oosterloo T, Morganti R, Alatalo K, Blitz L, Bois M, Bournaud F, Bureau M, Cappellari M, Crocker AF, Davies RL, Davis TA, de Zeeuw PT, Duc PA, Emsellem E, Khochfar S, Krajnović D, Kuntschner H, Lablanche PY, McDermid RM, Naab T, Sarzi M, Scott N, Trager SC, Weijmans AM, Young LM (2012) The ATLAS^{3D} project - XIII. Mass and morphology of H I in early-type galaxies as a function of environment. *MNRAS*422:1835–1862, DOI 10.1111/j.1365-2966.2012.20219.x, 1111.4241
- Sil'chenko OK, Chilingarian IV, Sotnikova NY, Afanasiev VL (2011) Large-scale nested stellar discs in NGC 7217. *MNRAS*414:3645–3655, DOI 10.1111/j.1365-2966.2011.18665.x, 1103.1692
- Sofue Y, Nakanishi H (2016) Three-dimensional distribution of the ISM in the Milky Way Galaxy. IV. 3D molecular fraction and Galactic-scale H I-to-H₂ transition. *PASJ*DOI 10.1093/pasj/psw062, 1604.05794

- Sofue Y, Honma M, Arimoto N (1995) The molecular front in galaxies. I. CO VS HI in position-velocity diagrams. *A&A*296:33
- Solomon PM, Rivolo AR, Barrett J, Yahil A (1987) Mass, luminosity, and line width relations of Galactic molecular clouds. *ApJ*319:730–741, DOI 10.1086/165493
- Sun M, Donahue M, Roediger E, Nulsen PEJ, Voit GM, Sarazin C, Forman W, Jones C (2010) Spectacular X-ray Tails, Intracluster Star Formation, and ULXs in A3627. *ApJ*708:946–964, DOI 10.1088/0004-637X/708/2/946, 0910.0853
- Sun Y, Xu Y, Yang J, Li FC, Du XY, Zhang SB, Zhou X (2015) A Possible Extension of the Scutum-Centaurus Arm into the Outer Second Quadrant. *ApJ*798:L27, DOI 10.1088/2041-8205/798/2/L27, 1412.2425
- Thilker DA, Bianchi L, Boissier S, Gil de Paz A, Madore BF, Martin DC, Meurer GR, Neff SG, Rich RM, Schiminovich D, Seibert M, Wyder TK, Barlow TA, Byun YI, Donas J, Forster K, Friedman PG, Heckman TM, Jelinsky PN, Lee YW, Malina RF, Milliard B, Morrissey P, Siegmund OHW, Small T, Szalay AS, Welsh BY (2005) Recent Star Formation in the Extreme Outer Disk of M83. *ApJ*619:L79–L82, DOI 10.1086/425251, arXiv:astro-ph/0411306
- Thilker DA, Bianchi L, Meurer G, Gil de Paz A, Boissier S, Madore BF, Boselli A, Ferguson AMN, Muñoz-Mateos JC, Madsen GJ, Hameed S, Overzier RA, Forster K, Friedman PG, Martin DC, Morrissey P, Neff SG, Schiminovich D, Seibert M, Small T, Wyder TK, Donas J, Heckman TM, Lee YW, Milliard B, Rich RM, Szalay AS, Welsh BY, Yi SK (2007) A Search for Extended Ultraviolet Disk (XUV-Disk) Galaxies in the Local Universe. *ApJS*173:538–571, DOI 10.1086/523853, 0712.3555
- Tosaki T, Kuno N, Onodera SM Rie, Sawada T, Muraoka K, Nakanishi K, Komugi S, Nakanishi H, Kaneko H, Hirota A, Kohno K, Kawabe R (2011) NRO M33 All-Disk Survey of Giant Molecular Clouds (NRO MAGiC). I. HI to H₂ Transition. *PASJ*63:1171–1179, 1106.4115
- van Dishoeck EF, Black JH (1988) The photodissociation and chemistry of interstellar CO. *ApJ*334:771–802, DOI 10.1086/166877
- van Gorkom JH (2004) Interaction of Galaxies with the Intracluster Medium. *Clusters of Galaxies: Probes of Cosmological Structure and Galaxy Evolution* p 305, astro-ph/0308209
- Vázquez RA, May J, Carraro G, Bronfman L, Moitinho A, Baume G (2008) Spiral Structure in the Outer Galactic Disk. I. The Third Galactic Quadrant. *ApJ*672:930-939, DOI 10.1086/524003, 0709.3973
- Verdugo C, Combes F, Dasyra K, Salomé P, Braine J (2015) Ram pressure stripping in the Virgo Cluster. *A&A*582:A6, DOI 10.1051/0004-6361/201526551, 1507.04388
- Vollmer B, Braine J, Combes F, Sofue Y (2005) New CO observations and simulations of the NGC 4438/NGC 4435 system. Interaction diagnostics of the Virgo cluster galaxy NGC 4438. *A&A*441:473–489, DOI 10.1051/0004-6361:20041389
- Walter F, Martin CL, Ott J (2006) Extended Star Formation and Molecular Gas in the Tidal Arms near NGC 3077. *AJ*132:2289–2295, DOI 10.1086/508273, astro-ph/0608169

- Walter F, Brinks E, de Blok WJG, Bigiel F, Kennicutt RC Jr, Thornley MD, Leroy A (2008) THINGS: The H I Nearby Galaxy Survey. *AJ*136:2563-2647, DOI 10.1088/0004-6256/136/6/2563, 0810.2125
- Wang QD, Owen F, Ledlow M (2004) X-Raying A2125: A Large-Scale Hierarchical Complex of Galaxies and Hot Gas. *ApJ*611:821–834, DOI 10.1086/422332, astro-ph/0404602
- Watson DM, Guptill MT, Buchholz LM (1994) Detection of CO J = 2 goes to 1 emission from the polar rings of NGC 2685 and NGC 4650A. *ApJ*420:L21–L24, DOI 10.1086/187153
- Watson LC, Martini P, Lisenfeld U, Böker T, Schinnerer E (2016) Testing the molecular-hydrogen Kennicutt-Schmidt law in the low-density environments of extended ultraviolet disc galaxies. *MNRAS*455:1807–1818, DOI 10.1093/mnras/stv2412
- Welch GA, Sage LJ (2003) The Cool Interstellar Medium in S0 Galaxies. I. A Survey of Molecular Gas. *ApJ*584:260–277, DOI 10.1086/345537, astro-ph/0210337
- Welch GA, Sage LJ, Young LM (2010) The Cool Interstellar Medium in Elliptical Galaxies. II. Gas Content in the Volume-limited Sample and Results from the Combined Elliptical and Lenticular Surveys. *ApJ*725:100–114, DOI 10.1088/0004-637X/725/1/100, 1009.5259
- Whitmore BC, McElroy DB, Schweizer F (1987) The shape of the dark halo in polar-ring galaxies. *ApJ*314:439–456, DOI 10.1086/165077
- Whitmore BC, Lucas RA, McElroy DB, Steiman-Cameron TY, Sackett PD, Olling RP (1990) New observations and a photographic atlas of polar-ring galaxies. *AJ*100:1489–1522, DOI 10.1086/115614
- Wolfire MG, Hollenbach D, McKee CF (2010) The Dark Molecular Gas. *ApJ*716:1191–1207, DOI 10.1088/0004-637X/716/2/1191, 1004.5401
- Wong OI, Kenney JDP, Murphy EJ, Helou G (2014) The Search for Shock-excited H₂ in Virgo Spirals Experiencing Ram Pressure Stripping. *ApJ*783:109, DOI 10.1088/0004-637X/783/2/109, 1401.6223
- Wong T, Blitz L (2002) The Relationship between Gas Content and Star Formation in Molecule-rich Spiral Galaxies. *ApJ*569:157–183, DOI 10.1086/339287, astro-ph/0112204
- Yagi M, Yoshida M, Komiyama Y, Kashikawa N, Furusawa H, Okamura S, Graham AW, Miller NA, Carter D, Mobasher B, Jogee S (2010) A Dozen New Galaxies Caught in the Act: Gas Stripping and Extended Emission Line Regions in the Coma Cluster. *AJ*140:1814–1829, DOI 10.1088/0004-6256/140/6/1814, 1005.3874
- Yasui C, Kobayashi N, Tokunaga AT, Terada H, Saito M (2006) Deep Near-Infrared Imaging of an Embedded Cluster in the Extreme Outer Galaxy: Census of Supernova-Triggered Star Formation. *ApJ*649:753–758, DOI 10.1086/506382, astro-ph/0606023
- Yasui C, Kobayashi N, Tokunaga AT, Terada H, Saito M (2008) Star Formation in the Extreme Outer Galaxy: Digel Cloud 2 Clusters. *ApJ*675:443-453, DOI 10.1086/524356, 0711.0257

- Young JS, Scoville NZ (1991) Molecular gas in galaxies. *ARA&A*29:581–625, DOI 10.1146/annurev.aa.29.090191.003053
- Young LM (2002) Molecular Gas in Elliptical Galaxies: Distribution and Kinematics. *AJ*124:788–810, DOI 10.1086/341648, *astro-ph/0205162*
- Young LM, Bureau M, Cappellari M (2008) Structure and Kinematics of Molecular Disks in Fast-Rotator Early-Type Galaxies. *ApJ*676:317-334, DOI 10.1086/529019, 0712.4189
- Young LM, Bureau M, Davis TA, Combes F, McDermid RM, Alatalo K, Blitz L, Bois M, Bournaud F, Cappellari M, Davies RL, de Zeeuw PT, Emsellem E, Khochfar S, Krajnović D, Kuntschner H, Lablanche PY, Morganti R, Naab T, Oosterloo T, Sarzi M, Scott N, Serra P, Weijmans AM (2011) The ATLAS^{3D} project - IV. The molecular gas content of early-type galaxies. *MNRAS*414:940–967, DOI 10.1111/j.1365-2966.2011.18561.x, 1102.4633